PRODUCTION, CHARACTERIZATION, AND ENVIRONMENTAL APPLICATIONS OF ENGINEERED CARBONS DERIVED FROM HYDROTHERMAL CARBONIZATION OF BIOMASS

By

JUNE FANG

A DISSERTATION PRESENTED TO THE GRADUATE SCHOOL
OF THE UNIVERSITY OF FLORIDA IN PARTIAL FULFILLMENT
OF THE REQUIREMENTS FOR THE DEGREE OF
DOCTOR OF PHILOSOPHY

UNIVERSITY OF FLORIDA

2016

To my family

ACKNOWLEDGMENTS

I would like to thank my advisor, Dr. Bin Gao, for providing me with his knowledge and guidance during the pursuit of my doctoral degree. I would also like to thank my committee members, Drs. Willie Harris, Greg Kiker, Zhaohui Tong, and Andrew Zimmerman for their support as well in conducting my research. I would also like to thank Billy Duckworth, Steve Feagle, Paul Lane, Orlando Lanni, and Daniel Preston for lending me their technical expertise in the lab. Thanks also to my fellow lab mates that I worked with in Dr. Gao's lab: Hao Chen, Anne Elise Creamer, Mandu Inyang, Ratna Suthar, Shensheng Wang, and Ming Zhang. Without the help of everyone, I would not be where I am right now.

TABLE OF CONTENTS

page

LIST OF TABLES

LIST OF FIGURES

LIST OF ABBREVIATIONS

AHC	Activated hydrochar
HTC	Hydrothermal carbonization
MB	Methylene blue
TGA	Thermogravimetric analysis

Abstract of Dissertation Presented to the Graduate School
of the University of Florida in Partial Fulfillment of the
Requirements for the Degree of Doctor of Philosophy

PRODUCTION, CHARACTERIZATION, AND ENVIRONMENTAL APPLICATIONS OF ENGINEERED CARBONS DERIVED FROM HYDROTHERMAL CARBONIZATION OF BIOMASS

By

June Fang

December 2016

Chair: Bin Gao
Major: Agricultural and Biological Engineering

Hydrochar has received increased attention recently as a potential agent for numerous environmental applications, including contaminant remediation. There is a need to understand how the properties of hydrochar and its derivatives vary with production conditions, and how their physicochemical properties affect their ability to adsorb contaminants from water. In this work, hydrochar was synthesized from waste biomass and tested for its ability to adsorb contaminants in water. First, hydrochar was produced from bagasse, hickory, and peanut hull feedstocks at several different temperatures, and the effects of the processing temperature on physicochemical characteristics and adsorption of methylene blue, lead, and phosphate were determined. Hickory and peanut hull resulted in higher hydrochar yields than bagasse. Among all the hydrochars, those made at the lowest temperature (200 °C) were the best for sorption of methylene blue and lead. None of the hydrochars were able to remove phosphate from solution. Next, hickory and peanut hull hydrochars were physically activated with CO_2 gas and chemically activated with KOH and H_3PO_4. Compared to their nonactivated counterparts, the activated hydrochars had higher surface areas,

especially those that were physically activated at 900 °C and chemically activated with H_3PO_4. The improved physicochemical characteristics led to greater methylene blue and lead adsorption rates compared to unactivated hydrochar. In summary, using hydrothermal carbonization to prepare engineered carbon (i.e., hydrochar and its derivatives) is a cost effective way to utilize waste biomass, especially when pristine hydrochar is modified to improve its physicochemical characteristics.

CHAPTER 1
OVERVIEW OF ENGINEERED CARBON DERIVED FROM HYDROTHERMAL CARBONIZATION OF BIOMASS

Introduction

Biomass is often thermally processed into biochar, a solid product that can be used for a variety of applications such as contaminant remediation, fuel, and amending soil for carbon sequestration purposes as well as to improve fertility and water retention (Inyang et al., 2010; Verheijen et al., 2009). Biochar is typically produced through pyrolysis, where dried biomass is heated in the absence of oxygen at high temperatures. However, hydrothermal carbonization (HTC) is being considered as an alternative method of processing biomass (Libra et al., 2011; Oliveira et al., 2013; Stemann et al., 2013). The solid created during HTC is called hydrochar in order to distinguish it from biochar (Libra et al., 2011).

During HTC, biomass is heated in an oxygen free environment in the presence of subcritical water and autogenous pressure in the range of 2-10 MPa (He et al., 2013; Mumme et al., 2011). HTC has several advantages over pyrolysis. Feedstocks with a high moisture content yield low amounts of solid material after drying, which makes them insufficient sources for pyrolysis (He et al., 2013). Therefore, a greater variety of feedstocks could be considered for processing into hydrochar since drying the feedstock is not necessary for HTC. Another advantage is that HTC yields higher amounts of char and uses lower amounts of energy than pyrolysis. This is due to the fact that the feedstock does not need to be dried, as well as lower operating temperatures for HTC compared to pyrolysis (Kang et al., 2012; Libra et al., 2011). HTC and pyrolysis generally use temperatures between 200-300 °C and 300-600 °C, respectively (Takaya et al., 2016). The lower operating temperature is due to the

activation temperatures of the chemical reactions that occur when the biomass is heated in the presence of liquid. When biomass is heated in the absence of oxygen, the physical structure is altered through reaction mechanisms such as hydrolysis, dehydration, decarboxylation, aromatization, and recondensation (Funke & Ziegler, 2010). While these reactions occur during both pyrolysis and HTC, hydrolysis is the predominant reaction during HTC, which has a lower activation energy than the other decomposition reactions (Libra et al., 2011).

Despite the fact that hydrochar can be used for the same purposes as biochar, it is still necessary to test their effectiveness in these applications and compare them to biochar. This is because the ratio of the types of chemical reactions affect the physical properties of the char (Kang et al., 2012; Libra et al., 2011). This overview compiles studies that have so far been conducted on the application of hydrochar and identifies knowledge gaps and future considerations in the study of hydrochar. A brief overview of the properties of hydrochar that distinguish it from biochar is also provided to give some insight on how they may be advantageous or disadvantageous for different applications.

Hydrothermal Carbonization

Hydrothermal Carbonization of Biomass

During the hydrothermal carbonization (HTC) of biomass, the biomass experiences structural rearrangement and parts of it degrade into liquid and gaseous products. The solid product that is created (hydrochar) has a chemical structure that is different from the feedstock. The difference in chemical structure is explained by the reaction mechanisms that occur during HTC, which include hydrolysis, dehydration, decarboxylation, aromatization, and recondensation (Funke & Ziegler, 2010). Although these processes generally occur in this order, they do not operate in a successive

manner; instead, they occur simultaneously during HTC and are interconnected with each other (Funke & Ziegler, 2010).

Out of all of these processes, hydrolysis has the lowest activation energy, so it is the first step to be initiated during HTC. Hydrolysis breaks down the structure of biomass through cleavage of ester and ether bonds of biomacromolecules with water molecules. This process creates (oligo-) saccharides and fragments of lignin that enter the liquid phase (Libra et al., 2011). The lignin fragments are then hydrolyzed into phenols, but the saccharides can continue to initiate other chemical pathways and products during HTC. The products created through these other mechanisms can also undergo hydrolysis (Kang et al., 2012).

Dehydration is the process where water is removed from the biomass matrix, causing hydroxyl groups to be eliminated. Decarboxylation is the removal of CO_2 from the biomass, eliminating carboxyl groups in the process. Aromatization occurs as a result of dehydration and decarboxylation. Double bonded functional groups such as C=O and C=C replace the single bonded hydroxyl and carboxyl groups in the biomass matrix (Sevilla & Fuertes, 2009). The furfural compounds generated by these two mechanisms then undergo hydrolysis, which further breaks them down into acids, aldehydes, and phenols. The acids that are generated then catalyze the release of inorganic elements from the biomass matrix (Fuertes et al., 2010).

The compounds created during the previously described mechanisms can undergo recondensation if they are highly reactive. Lignin fragments are highly reactive and condense easily, as well as aromatized polymers from cellulose degradation (Islam et al., 2015). The recondensation of HTC degradation products leads to the formation of

hydrochar (Libra et al., 2011). Degradation products from hemicellulose, however, stabilize lignin fragments and slow down condensation reactions significantly (Funke & Ziegler, 2010).

Chemical Changes that Occur in Biomass as a Result of HTC Reaction Mechanisms

Compared to raw biomass, hydrochars have a higher proportion of carbon and lower proportion of oxygen. This is mainly the result of the dehydration and decarboxylation processes, which remove hydrogen and oxygen from the solid in the form of H_2O and CO_2 (Funke & Ziegler, 2010). In addition to amount, the type of carbon found in hydrochar is also different from that of the raw biomass. Hydrochar contains more aromatic carbon than the raw biomass because dehydration and decarboxylation during HTC leads to the formation of aromatic carbon in the biomass (Libra et al., 2011). Hydrochar also has a lower ash content than biomass because the inorganic elements are released during degradation of the biomass and dissolved in the processing liquid during HTC (Fuertes et al., 2010). Sulfur and nitrogen contents are also lower in hydrochar because the nitrogen and sulfur oxides formed during HTC are dissolved in the processing liquid (Kang et al., 2012). All of these physicochemical changes can cause the effects between hydrochar and biochar in a specific application to be different from each other.

Properties of Hydrochar (vs Biochar)

Compared to biochar produced at typical temperature ranges, hydrochar has a lower C content since dehydration occurs in pyrolysis more so than it does in HTC (Libra et al., 2011). It also has a much lower ash content than biochar. While the inorganic elements (ash) in hydrochar enter the liquid phase during HTC, biochar

retains all of the original inorganic elements of the feedstock (Fang et al., 2015). As a consequence, hydrochar also is generally slightly more acidic than biochar, since the presence of ash increases pH (Parshetti et al., 2014). Biochar has a higher surface area and larger pore volume than hydrochar (Sun et al., 2014). The lower surface area of hydrochar is due to the persistance of the decomposition products on the surface of the hydrochar, which cause pore blockage (Fernandez et al., 2015).

Depending on the applications, the characteristics of hydrochar may be more desirable than that of biochar. For instance, a low ash content is desirable when the char is to be used as a fuel (Demirbas, 2007). Although high surface area and pore volumes are correlated with increased sorption ability, the lower ash content of hydrochar means that it may be a more suitable precursor for activated carbon, which has much higher surface area than biochar. Increasing soil pH is one of the positive effects of biochar when used as a soil amendment (Van Zwieten et al., 2010), and hydrochar may be used to decrease the pH of soils with high basicity.

Potential Applications of Hydrochar

Soil Amendment

Sequestration for climate change mitigation

Biochar is known to be a good material for carbon sequestration for climate change mitigation, as pyrolysis processes biomass into a more recalcitrant form. Likewise, hydrochar could be used for the same purposes if shown to be similarly recalcitrant. The GHG fluxes have been studied in soil for greenhouse gases such as N_2O, CO_2, and CH_4 (Kammann et al., 2012; Malghani et al., 2013). Generally, hydrochar has been found to be ineffective for climate change mitigation. Corn hydrochar was found to increase CO_2 and CH_4 emissions from soil, although it did

decrease N_2O compared to unamended soil. In contrast, corn biochar was able to decrease CO_2 emissions, had no significant effect on CH_4, and had intermediate levels of N_2O (Malghani, 2013). In experiments on beet chip and bark hydrochars, N_2O emissions decreased, but increased significantly when N fertilizer was present (Kammann et al., 2012). The increase in CO_2 emissions was due to the lesser stability of the C in the hydrochar as well as the fact that it stimulated more microbial activity than biochar as a result of its higher degradability (Kammann et al., 2012; Schimmelpfennig et al., 2014).

Fertility

Although hydrochar has a low nutrient content and cannot be used as a fertilizer by itself, it may be added to soil to enhance the effects of fertilizer by reducing the amount of fertilizer that is lost through surface run-off (Beck et al., 2011). The nutrients are sorbed into the pores on the surface of the char, which then slowly release the nutrients into the soil over time for plant uptake (Yao et al., 2013a). As a result, biochar has been found to have a synergistic effect with fertilizers on enhancing plant growth due to more of the fertilizer being retained in the soil in the presence of biochar (Glaser et al., 2002; Rondon et al., 2007). Likewise, this property has been investigated in hydrochar. When hydrochar is added to soil, it was found that it improved yield for phaseolus beans and barley, but decreased yield for leek (Bargmann et al., 2014). In another study, beer draff and sugar beet pulp hydrochars were found to reduce the growth of sugar beet growth (Gajic & Koch, 2012). The decrease in plant growth was attributed to N immobilization that was the result of decomposition activity from the hydrochars (Bargmann et al., 2014; Gajic & Koch, 2012).

Water retention

Adding maize hydrochar to soil increases the amount of water that can be retained by the soil, although this improvement is observed only in sandy soils, which have a low available water capacity (AWC). Soils with high AWC such as those with high organic matter content did not show as dramatic an improvement in their physical properties (Abel et al., 2013). The addition of hydrochar to soil decreases the bulk density of soil and increases total pore volume, allowing more water to be retained by soil (Abel et al., 2013). However, hydrochar is not as effective as biochar in improving the water holding capacity of soil, as hydrophobicity was observed in some areas of the hydrochar. The water repellency was due to fungal colonization of the surface of the hydrochar, since hydrochar is more prone to biological degradation than biochar (Abel et al., 2013).

Energy from Hydrochar

Hydrochar can be used directly as a solid fuel that can be burned for energy or it can be used to synthesize fuel cells, electrode supercapacitors, and batteries as a medium for converting and storing energy (Ding et al., 2012; He et al., 2013; Reza et al., 2012). It is considered to be a good potential solid fuel due to its low ash content; the inorganic minerals in the biomass enter the processing liquid during the HTC process, while in pyrolysis, the nutrients are retained in the biochar (Fang et al., 2015). Materials with lower ash content would burn cleaner and more efficiently since the presence of inorganic minerals such as Si, K, Na, S, Cl, P, Ca, Mg, and Fe that are involved in reactions during biomass combustion causes toxic emissions as well as fouling, slagging, and corrosion in combustors (Demirbas, 2007).

Solid fuel

Raw biomass by itself is a poor quality fuel due to its low bulk density and ash and moisture content. It is thus typically processed into pellet form to increase its bulk density in order to reduce storage and transportation costs. However, some problems that arise from long term storage include moisture uptake and disintegration, both of which are conducive to microbial and biochemical activity (Lehtikangas, 2000). In addition, the act of compressing the raw biomass into a dense enough form is an energy intensive process. In one study, hydrochar pellets produced from pinewood sawdust, rice husk, coconut fiber, and coconut shell were tested for their density, maximum compressive force, and tensile strength (Liu et al., 2014). The densities of these pellets were 180-482 % higher than those of the corresponding raw pellets, with raw pellets ranging from 984-1141 kg/m^3 and hydrochar pellets ranging from 1153-1334 kg/m^3. Maximum compressive force and tensile strength ranged from 1049-1867 N and 2.97-7.5 MPa and 246-990 N and 0.96-3.91 MPa for the hydrochar and raw pellets, respectively. The HHV (higher heat value) has been found to be comparable to that of lignite coal, ranging from 15.08-21.74 MJ/kg (Liu et al., 2014). In another study, pine wood hydrochar pellets were found to have a mass density of 1468.2 kg/m^3 and HHV of 26.4 MJ/kg compared to values of 1102.4 kg/m^3 and 20.7 MJ/kg for raw pellets (Reza et al., 2012). In both studies, the hydrochars also had reduced moisture uptake by the pellets as a result of its hydrophobic nature.

Other studies have focused on the combustion characteristics of hydrochar used as a solid fuel. In a study on sewage sludge hydrochar, thermogravimetric analysis was utilized to analyze its combustion behavior (He et al., 2013). The hydrochar took longer than the raw sewage sludge to burn completely, and decomposition occurred at two

stages. On the other hand, the raw sewage sludge only had one decomposition stage, meaning that it was unstable and burned out quicker, leading to a large loss in heat. The raw sludge also had higher toxic emissions. The improved combustion was attributed to the higher fixed carbon and lower volatile matter of the hydrochar due to removal of nitrogen, sulfur, and heavy metals during the HTC process. The decrease in H/C and O/C ratios meant a loss of oxygenated functional groups on the surface, increasing the hydrophobicity of the hydrochar, as oxygen functional groups are hydrophilic. This is also a favorable characteristic during combustion, as less water droplets are taken up by the hydrochar from the atmosphere (He et al., 2013).

Hydrochar as capacitors

Rice husk hydrochar was found to be a good capacitor when combined with nickel. The nickel acted as a graphitization catalyst, which improved the specific capacity of hydrochar by 149%. The hydrochar/nickel composite had a specific capacitance of 174.5 F g^{-1}, which was higher than that of an activated carbon/nickel composite (Ding et al., 2012). In another study, N-doped soybean residue hydrochars were also found to have values of specific capitance: 250-260 F g^{-1} in H_2SO_4 and 176 F g^{-1} in Li_2SO_4 (Ferrero et al., 2015).

Low-Cost Adsorbent

Hydrochar has been found to be a low cost adsorbent for contaminants in aqueous solutions, and a range of sorption ability has been found for hydrochar. The differences in sorption capacity depended on the processing conditions (such as time and temperature) and feedstocks that were used, as well as the contaminant that was being tested for adsorption. In general, pristine hydrochars are poor sorbents, which is due to a variety of factors. Hydrochar has a high volatile organic compound (VOC)

content, which may leach into the water, thus contributing its own contamination. Although many of the volatile compounds are water soluble, oftentimes, rinsing the hydrochar is not enough to remove the VOCs (Bargmann et al., 2013; Buss & Masek, 2014). Hydrochar also has poor characteristics for sorption: its low surface area and pore volume provide less sorption sites for contaminants, and its negative surface charge is unconducive to adsorbing negatively charged substances (Fang et al., 2015). Therefore, modifying the hydrochar through activation can provide the desired characteristics for contaminant remediation.

Heavy metal removal

Activating hydrochars with chemicals was shown to improve their sorptive abilities for a variety of heavy metals. KOH chemically modified wheat straw, corn stalk, and sawdust hydrochar were found to be effective for sorption of cadmium in aqueous solutions. These hydrochars had cadmium sorption capacities that were 2-3 times higher compared to that of their unmodified counterparts (30.40-40.78 mg g^{-1} vs. 13.92-14.52 mg g^{-1}). The improved sorption ability was attributed to the oxygenated functional groups that were formed on the surface of the hydrochar after being modified with KOH (Sun et al., 2015). Peanut hull hydrochars were found to have a higher sorption capacity for lead when washed with H_2O_2. The H_2O_2 modified hydrochar had a sorption rate of 22.82 mg g^{-1} while the unmodified hydrochar was only able to sorb 0.88 mg g^{-1} (Xue et al., 2012). The increase in sorption rate was also attributed to the increase in oxygenated surface functional groups after H_2O_2 modification.

Phosphate removal

Although hydrochar has an affinity for dyes and metals, it does not for anionic substances, which is due to its negative surface charge (Fang et al., 2015). In order to

increase its ability to sorb anionic compounds, the surface of hydrochar needs to be modified so that it would possess a positive charge. Modifying hydrochar with lanthanum is one of the methods that can be used to improve its ability to adsorb phosphate (Dai et al., 2014). Lanthanum is often used to modify materials such as silica for phosphate removal purposes, as it attaches easily to oxygenated surface functional groups of the material that it is being used to modify. A one pot hydrochar synthesis experiment was conducted to create lanthanum doped rice straw hydrochar. The resulting material was found to have a high affinity for phosphate and was able to adsorb 61.57 mg P g^{-1}, while pristine hydrochars had adsorption rates ranging from 0-30 mg P g^{-1} (Dai et al., 2014; Takaya et al., 2016).

Organic removal

Hydrochar has been tested for its ability to adsorb organics ranging from dyes, pharmaceuticals, and pesticides. Orange peel hydrochar was modified with H_3PO_4, and it was tested for its ability to adsorb three different pharmaceuticals: salicylic acid, flurbiprofen, and diclofenac sodium (Fernandez et al., 2015). Activation with H_3PO_4 was able to increase sorption capacity of the hydrochar by almost ten times for all three pharmaceuticals. Hydrochar has also been found to be good for adsorbing dyes, especially after undergoing chemical activation. Pine needle hydrochar had a sorption capacity for malachite green of 52.91 mg g^{-1} and 97.08 mg g^{-1} when modified with H_2O_2 (Hammud et al., 2015).

Pathogen removal

Most studies on the usage of hydrochar for contaminant remediation is conducted on organics and heavy metals, although a few have been conducted on pathogens. Maize hydrochar was found to be effective for the removal of *E. coli* in sand

columns amended at a rate of 1.5% on a w/w basis, especially when activated with KOH. Raw and KOH activated maize hydrochars removed *E. coli* at rates of 72% and 93%, respectively. The higher rate of the modified hydrochar is due to KOH improving the porous surface structure and decreasing negative surface charges on the hydrochar, as *E. coli* has a negative surface charges. The *E. coli* that was removed was also well attached to the hydrochar (Chung et al., 2014). Adenovirus and rotavirus were able to be removed from water at rates of 99.6% in sand columns amended with sewage sludge hydrochar because the hydrophobic and porous natures of the hydrochars provided favorable attachment sites for the virus (Chung et al., 2015).

Medical Applications

Flourescent quantum dots are an emerging form of medical imaging for detection of disease at the cellular level. Quantum dots produced from silk hydrochar have been tested for their potential to be used in organ imaging due to the lower amount of heavy metals than quantum dots synthesized from other materials. Its good hemocompatibility, low toxicity, high cellular uptake, and localization confirmed that it is a safe and effective material to be used in the body. It also displayed a strong blue fluorescence under certain wavelengths, making it a suitable substitute for dyes that are traditionally used in medical imaging (Ruan et al., 2014).

Knowledge Gaps & Future Directions

The effectiveness of hydrochar compared to biochar depends on the application it is being used in and the type of feedstock used. For many of the applications discussed, hydrochar was found to be less effective than biochar in unmodified form. Characteristics that are negative for one type of application may be advantageous for others, such as hydrophobicity, which is desirable for fuel but not when the hydrochar is

to be used as a soil conditioner to improve water retention. Once the behavior and characteristics of hydrochar are identified under carefully controlled laboratory conditions, future directions on study could involve the use of hydrochar on large scale, real world applications. In addition, activation of hydrochar should be further investigated, as studies conducted so far show that activation significantly improves its ability to adsorb contaminants from water, with the added advantage of hydrochar being a more energy efficient precursor for activated carbon than biochar. There are numerous methods of activation, and a variety of methods should be tested to determine their effects on the sorption ability of hydrochar.

Research Objectives

The work in this dissertation was planned for the purpose of improving the ability of hydrochar to remove contaminants from water. It is hypothesized that physical and chemical activation will greatly improve the physicochemical properties of hydrochar, while creating a lower cost sorbent at the same time.

Hypothesis 1

Hydrochar has comparable physical and chemical properties to biochar and thus can be used as soil amendment and adsorbent.

Objective 1

Synthesize hydrochars from a range of feedstock types and characterize their physicochemical properties. The specific objectives of this study were to:

- Hydrothermally carbonize bagasse, hickory, and peanut hull feedstocks at different temperatures (200, 250, and 300 ºC)
- Characterize them for mass and C yield, surface area, pore volume, elemental content, pH, zeta potential, and thermal stability

- Conduct preliminary experiments on sorption of methylene blue, lead, and phosphate
- Conduct seed germination studies to assess toxicity on plants

Hypothesis 2

Physical activation of hydrochar with CO_2 will improve the ability of hydrochar to adsorb lead and methylene blue due to increases in surface area and pore volume.

Objective 2

Physically activate hydrochar and conduct prelimnary batch sorption experiments to determine if activation improves its ability to adsorb MB and lead from water. The specific objectives of this study were to:

- Physically activate (via thermal treatment with CO_2) hickory and peanut hull hydrochars at different combinations of time (1 and 2 h) and temperature (600, 700, 800, and 900 °C)
- Physicochemically characterize the resulting AHCs for their surface area, pore volume, and CHN content
- Conduct batch sorption experiments to test the ability of the resulting AHCs to adsorb dyes (methylene blue) and heavy metals (Pb, Cu, and Cd) from water

Hypothesis 3

Chemical activation of hydrochar with H_3PO_4 and KOH will improve the ability of hydrochar to adsorb contaminants due to increase in surface area and pore volume.

Objective 3

Chemically activate hydrochar and conduct batch sorption experiments to determine if activation improves its ability to adsorb contaminants from water. The specific objectives of this study were:

- Activate hickory and peanut hull hydrochars with H_3PO_4 and KOH
- Physicochemically characterize the resulting AHCs for their surface area, pore volume, and CHN content
- Conduct batch sorption experiments to test the ability of the resulting AHCs to adsorb dyes (methylene blue) and heavy metals (Pb) from water

CHAPTER 2
HYDROCHARS DERIVED FROM PLANT BIOMASS UNDER VARIOUS CONDITIONS: CHARACTERIZATION AND POTENTIAL APPLICATIONS AND IMPACTS

Introduction

Biochar is a pyrolysis product that can be utilized for multiple environmental applications, including contaminant remediation, soil amelioration, and carbon sequestration (Mohan et al., 2014; Zimmerman et al., 2011). Chars created through hydrothermal carbonization (HTC), also known as hydrochars, can be used for the same purposes as biochars but differ in several aspects (Libra et al., 2011; Xue et al., 2012). Hydrolysis, the first step in HTC, requires lower activation energy than many of the dry pyrolysis decomposition reactions (Funke & Ziegler, 2010; Reza et al., 2014). The feedstocks of HTC do not need to be dried and thus it requires less energy inputs (Libra et al., 2011). Nutrient-rich soluble materials of possible high value are a byproduct of hydrochar production whereas gases and bio-oils are produced during biochar production that may be difficult to utilize. Finally, hydrochars have been found to be more efficiently pelletized than biochars, which increases their energy density, reducing transportation costs and handling difficulties (Reza et al., 2012).

Despite these advantages, hydrochar has not received nearly as much research attention as biochar. Until recently, research on the hydrothermal processing of feedstocks has mostly focused on the resulting liquid products (Alvira et al., 2010). As with biochar, it has been found that feedstock and processing conditions greatly affect hydrochar properties (Berge et al., 2011; Kang et al., 2012; Kim et al., 2014; Sun et al., 2014). Similar to biochar, hydrochar yield decreased with increasing highest treatment temperature (HTT), but also varied with the type of feedstock. For example, hydrochar created from waste materials, including waste paper, food waste, mixed municipal solid

waste, and anaerobic digestion waste, had yields ranging from 29% to 63% (Berge et al., 2011), pinewood meal had yields between 50% and 60% for HTTs ranging from 225 °C to 265 °C (Kang et al., 2012), and anaerobically digested sludge had yields ranging from 80.4% to 93.9% for HTTs from 180 °C to 250 °C (Kim et al., 2014).

While surface area is directly correlated with HTT for dry pyrolysis chars, mixed results are observed for hydrochar. Pinewood hydrochar showed an increase in surface area from 9.65 m^2 g^{-1} to 20.43 m^2 g^{-1} when the HTT was increased from 250 °C to 300 °C (Liu & Zhang, 2009). However, surface area decreased as HTT increased for hydrochar made from urban food waste and anaerobically digested corn silage (Mumme et al., 2011; Parshetti et al., 2014). In biochar, carbon content increases with increasing HTT, while hydrogen and oxygen decrease (Sun et al., 2014). Trace mineral contents also increase with higher HTT and thus become more alkaline as well (Ding et al., 2014a; Sun et al., 2014). Hydrochars tend to be more acidic than biochar due to their lower trace element contents (Parshetti et al., 2014; Sun et al., 2014).

Because the elemental composition and physicochemical properties of hydrochars vary with production conditions, it is important to optimize the production conditions of hydrochar to its intended uses. While a number of studies have compared hydrochars to biochars for a specific applications, few comprehensive studies have compared hydrochars created under a range of processing conditions and testing them for a variety of applications (Libra et al., 2011). Even fewer studies have examined the potential of hydrochars to sorb environmental contaminants and thus be used for environmental remediation.

The overarching objective of this study was to determine how feedstock and production temperature affect the physicochemical properties, potential applications, and potential impacts of hydrochar, and thus to determine the optimal processing conditions for effective usage in multiple purposes. Hydrochars were produced from bagasse, hickory, and peanut hull, each at 200 °C, 250 °C, and 300 °C, and their basic physical and chemical properties were determined. To test the ability of hydrochars to sorb organic, cationic, and anionic contaminants, laboratory batch sorption were conducted with methylene blue, lead, and phosphate, respectively. Growth studies were also conducted to investigate whether or not these hydrochars are safe for environmental applications.

Materials and Methods

Hydrochar Production

Three different feedstocks were used: sugarcane bagasse (B), hickory (H), and peanut hull (P). The feedstocks were milled to particle sizes of 0.5–1 mm and added to a 500 mL stainless steel pot so that there was about one inch of space between the feedstock and the top of the autoclave. Deionized (DI) water was added to ensure that the feedstocks were submerged. There were 40 g of bagasse, 50 of hickory, and 55 g of peanut hull with 310 mL, 290 mL, and 313 mL of water, respectively. The pots were heated on a hotplate to 200 °C, 250 °C, and 300 °C for 6 h, respectively. The pots were then allowed to cool to room temperature. The resulting hydrochars were then isolated by filtration using 0.45 µm filter paper (Whatman), washed for 1 h by submersion in tap water and 10 min in DI water to remove water soluble volatile matter, and oven dried for 24 h at 70 °C. The hydrochar samples obtained were labeled as B200, B250, B300,

H200, H250, H300, P200, P250, and P300, respectively, based on their feedstock type and processing temperature.

Characterization of Hydrochar Properties

A CHN Elemental Analyzer (Carlo-Erba NA-1500) was used to determine the carbon, hydrogen, and nitrogen contents of the hydrochars. Inorganic elemental concentrations were measured after dry ashing 0.2 g of each hydrochar in a muffle furnace for 2 h at 550 °C. A 5% HNO_3 solution was added to each of the ashed samples, and the solutions were measured for multiple trace elements through ICP analysis (ICP-AES, Perkin Elmer Optima 2100 DV). Oxygen content was calculated as the difference between the original dried sample weight and the sum of weights of all the measured elements.

The surface areas (SA) and pore volumes (PV) of the samples were measured by N_2 and CO_2 sorption on a Quantachrome Autosorb I, with N_2 at 77 K and CO_2 at 273 K, respectively. Samples were de-gassed under vacuum at least 24 h at 180 °C prior to analysis. SA-N_2 was calculated according to BET theory using adsorption data in the 0.01 – 0.3 relative pressure range, while SA-CO_2 used the <0.02 range relative pressure data and were interpreted using canonical Monte Carlo simulations of the non-local density functional theory. Because N_2 is kinetically impeded from entering micropores (<1 nm), SA-N_2 represents only mesopore-enclosed surfaces (2–50 nm). SA-CO_2 includes micropores because CO_2 diffusion is less kinetically limited and BC is more flexible at 273 K. Mesopore volumes (PV-N2) were calculated using Barrett–Joyner–Halenda (BJH) theory and micropore volumes (PV-CO2) using the Grand-Canonical-Monte-Carlo (GCMC) method and assuming slit-shaped pores and an equilibrium model.

The thermal stability of the hydrochars were measured with a thermogravimetric analyzer (Mettler Toledo) using a heating rate of 10 °C/min from 25 °C to 700 °C under a steady stream of airflow at 50 mL/min. Ash content was determined as the mass left over after this treatment.

To determine pH, 1 g of each hydrochar mixed with 20 mL of DI water was shaken on a mechanical shaker for 2 h and then measured with a pH meter (Fisher Scientific Accumet Basic AB15). Zeta potential was measured by mixing 10 mg of hydrochar with 100 mL DI water and sonicating the mixture for 3 h to break up the hydrochar particles into smaller fractions. The resulting solution was analyzed with a Brookhaven ZetaPlus zeta potential analyzer.

Batch Sorption Experiments

Three different contaminants were tested: methylene blue (20 ppm), lead (20 ppm), and phosphate (50 ppm). All chemicals used were ACS certified and obtained from Fisher Scientific and solutions were prepared using DI water (Nanopure water, Barnstead). Mixtures of 30 mL of each solution and 0.1 g of hydrochar in digestion vessels were shaken on a mechanical shaker at 40 rpm for 24 h. The solutions were then immediately filtered through 0.45 μm filter paper (Whatman). Lead and phosphate contents were analyzed using the ICP spectroscopy, and methylene blue was measured with a UV spectrometer at a wavelength of 665 nm.

Seed Germination and Seedling Growth

To test the effects of hydrochars on seed germination and growth, filter paper (Whatman 42 Ashless) was cut to fit snugly in the bottom of plastic beakers. Then 0.2 g of each hydrochar was sprinkled on the filter paper along with 20 brown top millet seeds and 3 mL of DI water. In the control group, 20 brown top millet seeds and 3 mL of DI

water were sprinkled on the filter paper. The beakers were covered with aluminum foil and kept at room temperature in the dark for 72 h. Afterwards, the number of seeds that germinated was counted and the lengths of the roots and shoots of each germinated seedling were recorded in a fully extended position.

Results and Discussion

Hydrochar Production Rates

Hydrochar yield ranged from 26.8% to 54.6% from the initial dry weight of the feedstocks (Table 2-1). For all feedstocks tested, hydrochar yield decreased with increasing production temperature. Sugarcane bagasse had the lowest char yield for all three temperatures. This is likely because a greater degree of biomass dissolution occurred at higher temperatures; more volatilization loss of biomass occurs at higher pyrolysis temperatures, decreasing biochar yield (Liao et al., 2013; Zimmerman, 2010). When the pyrolysis temperature was the same, hickory had the highest char yield percentage among the three feedstocks for 200 °C and 250 °C, while peanut hull had the highest char yield percentage for 300 °C. The lower yield of sugarcane bagasse for all three temperatures is likely related to its lower lignin content than woods and husks (Demirbas, 2001). Lignin has a stable phenolic structure that allows it to resist breaking down into liquid and gaseous fractions. For example, pure lignin was previously shown to have the highest char yield during HTC compared to pure cellulose and pine wood meal (Kang et al., 2012). Furthermore, the high cellulose content of bagasses also caused its hydrochar yield to decrease at a greater rate from 200 °C to 250 °C than that of hickory and peanut hull.

Surface Area and Pore Volume

Hydrochar surface areas and pore volumes (Table 2-1) were low (mesopore SA < 10 m^2 g^{-1} and micropore SA < 150 m^2 g^{-1}), similar to that of the original biomass and pyrolytic biochars made at low temperatures (<400 °C) (Zimmerman, 2010). Hydrochars with the highest surface area and pore volume were those produced at 200 °C regardless of feedstocks (Table 2-1). This is different from dry pyrolysis chars, where production temperature is often positively correlated with surface area and pore volume (Kloss et al., 2012). The decrease in surface area and pore volume as HTT increased was a phenomenon observed in oil palm stone biochars, where surface area steadily increased from 400 °C to 800 °C before decreasing (Guo & Lua, 1998). In pine biochar, surface area also began to decrease as HTT went over 750 °C (Brown et al., 2006). The decrease in surface area is due largely to the pore wall collapse as a result of deformation, melting, and fusion at high HTTs, which occurs at a lower temperature threshold for hydrochars than it does for dry pyrolysis chars, probably because the HTC pressure increases exponentially with the temperature (Wagner, 1973).

Elemental Composition

Carbon content was directly related, and oxygen and hydrogen contents were indirectly related to temperature for all feedstocks (Table 2-2). This is consistent with results observed previously for both biochars and hydrochars (Qian et al., 2013; Sun et al., 2014). At higher temperatures, cleavage and cracking of weak oxygen and hydrogen bonds occur during pyrolysis, resulting in carbon content increase in the biochar (Qian et al., 2013). In the case of hydrochars, it is likely that O and H-containing chemical moieties are more soluble and thus preferentially lost at higher temperatures and pressures.

The O/C and H/C of the hydrochars decreased with increasing temperature (Table 2-2), suggesting that higher temperature hydrochars have relatively high levels of aromaticity and will thus be of greater stability when applied to soils (Bai et al., 2014). Previous studies have shown that biochars with an O/C ratio below 0.2 will have a half-life of at least 1000 years (Spokas, 2010). It might follow that the 300 °C bagasse hydrochars (B300) produced in this work can be similarly used to enhance soil C sequestration.

The high O/C of hydrochars obtained at low HTC temperatures indicate greater abundances of oxygenated surface functional group such as hydroxyl, carboxylate, and carbonyl groups (Joseph & Lehmann, 2009). These functional groups yield a greater cation exchange capacity (CEC), which is beneficial for nutrient retention in soils and sorption of positively charged contaminants such as heavy metals (Inyang et al., 2015; Uchimiya et al., 2011; Xue et al., 2012). Thus, low temperature hydrochars may be useful for soil amelioration and contaminant remediation purposes.

C/N ratios ranged from 37 to 392 (Table 2-2). The relationship between HTT and C/N ratio was inconsistent. For bagasse hydrochar, C/N ratio decreased with increasing HTT. Hickory 250 °C hydrochar, however, had the lowest C/N ratio, while C/N ratio in peanut hull experienced little change with HTT. In any case, hydrochars are not likely to be significant sources of N to microbes or plants (Rondon et al., 2007; Zhou et al., 2013).

All of the hydrochars were low in minor and trace element concentrations (less than 1% for the elements tested, Table 2-2). Thus, they would not likely be useful as direct sources of nutrients, such as K, Ca, and P. The processing liquid was rich in

nutrients as most of the nutrients in the biomass feedstocks were released during the HTC process and thus might be applied to agricultural land to fertilize crops (Table 2-3). Furthermore, when hydrochars are applied with commercial fertilizers to soils, they may retain nutrients from leaching and improve soil fertility as well as promote carbon sequestration (Libra et al., 2011). Additionally, hydrochars with low inorganic element contents could be “clean” sorbents in aqueous solutions, as they will not alter the chemistry of the solution being remediated.

pH and Zeta Potential

Consistent with results of previous studies (Fuertes et al., 2010; Liao et al., 2013), all the hydrochars were slightly acidic (Table 2-1). At all temperatures, hydrochars produced from bagasse are more acidic than those from hickory and peanut hull. The pH of the hydrochars has been found to be controlled by the inorganic mineral contents of the feedstock (Parshetti et al., 2014). As the mineral content of these samples was found to be so low, however, it may also be dependent upon their organic acid content as has been suggested previously for low temperature biochars (Mukherjee et al., 2011). While higher temperature chars tend to be alkaline, the acidity of the hydrochars are similar to that of low temperature biochars, which have both lower mineral contents and higher levels of volatile organic matter (Mukherjee et al., 2011). Thus, while hydrochars would not be useful for neutralizing soil acidity, their pH buffering capacity may help a soil to retain nutrients.

The zeta potential for all of the hydrochars was moderately negative (Table 2-1), indicating that they have negative surface charges (Yuan et al., 2011). Thus, hydrochars may be suitable as sorbents of positively charged ions, such as heavy metals. No specific pattern was observed for zeta potential measurements of the

hydrochars, although zeta potentials of those derived from bagasse produced at 250 °C and peanut hull at 300 °C were the lowest.

Thermogravimetric Analysis (TGA)

Thermal decomposition of all the hydrochars began at around 300 °C and was complete by about 550 °C (Figure 2-1). As one would predict, thermal stability increased with HTT for all three feedstocks. Although peanut hull was the most thermally stable, the differences in thermal stability among the feedstocks was not as distinct as it generally is for biochar (Sun et al., 2014).

Previous studies have shown that thermal stability is a good predictor of biogeochemical stability of biochars (Yao et al., 2014; Zhang et al., 2012b). The TGA results suggest that hydrochars will be likely to remain stable in the soil if used for carbon sequestration purposes as they will be more resistant to microbial oxidation (Harvey et al., 2012). If thermal stability is used as a predictor for biogeochemical stability, hickory and bagasse hydrochars do not show any notable improvement in recalcitrance when HTT is increased to 300 °C.

Sorption of Contaminants

Results from the batch sorption experiments showed that the higher the HTC temperature, the lower the sorption rate for lead and methylene blue onto the hydrochars, regardless of the feedstock types (Figure 2-2). Hickory hydrochars were most effective at sorbing the two contaminants and H200 and H250 removed nearly 100% of methylene blue from the solution. The higher sorption rates of lead and methylene blue at lower temperatures correspond with the fact that lower temperature hydrochars have higher surface areas. The only exception was P300, which showed lower sorption rates than P250, despite a higher surface area. This could be explained

by the lower oxygen content of P300. The higher oxygen content in P250 means that there are more oxygen based functional groups for cations to be adsorbed to. Previous studies have demonstrated that oxygen containing functional groups such as carboxyl and hydroxyl groups play an important role in controlling the sorption of lead and methylene blue on biochar and other carbon materials (Ding et al., 2014b; Inyang et al., 2014; Mohan et al., 2014). In this work, it is anticipated that the sorption of lead by the hydrochars was mainly attributed to the electrostatic (interaction with negatively charged sites) and complexation (with carboxyl and hydroxyl groups) mechanisms (Ding et al., 2014a; Inyang et al., 2014; Inyang et al., 2015), while the sorption of methylene blue by the hydrochars could be mainly controlled by the electrostatic interactions between the cationic contaminant and the negative charge of the carbon surface (Ding et al., 2014b; Inyang et al., 2014).

None of the hydrochars, however, showed significant affinity for phosphate (Figure 2-2). This is due to the fact that they have negative surface charges, which repel negatively charged compounds such as phosphate (Zhang & Gao, 2013; Zhang et al., 2013; Zhang et al., 2012a). Several studies have shown that the repulsive electrostatic interactions can reduce the sorption of phosphate ions onto negatively charged carbon surfaces (Yao et al., 2013a; Yao et al., 2013b; Zhang et al., 2012a).

Hydrochars derived from bagasse and peanut hull at 250 °C displayed a more drastic decrease in sorption ability from those produced at 200 °C, while this pattern did not become apparent in those derived from hickory. Compared to hickory, the peanut hull char’s surface area decreased significantly when the target heating temperature was increased from 200 °C to 250 °C. Bagasse did not experience a dramatic decrease

in surface area, but the decreased sorption ability can be explained by the oxygen contents of the chars – from 200 °C to 250 °C, the oxygen content decreased more for bagasse than it did for hickory, by 6% and 2%, respectively.

Seed Germination and Growth

None of the hydrochars showed any statistically significant effects on seed germination rates of brown top millet (Figure 2-3). The hydrochars used in our experiment had been washed with DI water. These results are consistent with those shown in previous studies conducted on hydrochar application to spring barley, which indicated that phytotoxic volatile compounds found in unwashed hydrochar were responsible for the reduced seed germination rate (Bargmann et al., 2013). When seeds germinated on water washed hydrochars, the difference in germination rate was insignificant compared to control treatments. In the same study, biochar was found to have no harmful effects on seed germination because much of the volatile matter was evaporated during pyrolysis (Bargmann et al., 2013). In the studies of chars produced from dry pyrolysis, higher temperature biochars were found to have a more positive effect on plant growth than lower temperature biochars. The lower temperature biochars had volatile compounds on the surface that blocked the pores on the char, but after washing, no difference was observed (Buss & Masek, 2014).

Hydrochars derived from lower temperature tended to be better for seedling growth than those produced at higher temperatures (Figure 2-4). Among the entire tested samples, the group with B200 had the longest average root and shoot lengths. ANOVA tests were conducted, and hydrochar amendment was not observed to have a significant effect on shoot lengths. However, the results showed that the root length of seedlings produced with H250 and P300 were significantly reduced compared to that of

the control and other hydrochar treatments (Figure 2-4). In addition to the physical and chemical properties, it is possible that some unknown factors may affect seedling growth. For example, volatile matter was able to be removed from the hydrochars through prewashing treatment; however, the tars, which the higher temperature hydrochars had a higher content of, are not water soluble. Tar remnants on the hydrochar may affect the growth of the seedlings. Nevertheless, our results showed that seedlings grown with hydrochars produced at 200 °C were generally comparable to those produced from the control treatment.

Conclusions

Hydrothermal carbonization provides an alternative to dry pyrolysis to convert waste biomass to a useful product that can be used for soil amelioration or contaminant remediation. In addition to higher yields and lower energy inputs during its production, the hydrochars produced by HTC had unique physical characteristics and good ability to sorb aqueous cationic contaminants. None of the hydrochars had any negative effects on seed germination and shoot growth, though two of the higher temperature hydrochars showed a tendency to decrease root growth.

While the higher temperature chars were more thermally stable than lower temperature chars, the difference was not as pronounced as it is in biochars. Because hydrochars created at lower temperature (200 °C) require less energy to produce and showed higher yields, better sorption ability, and no negative effect on plants, low temperature HTC of plant biomass should be recommended for most environmental remediation and soil amendment purposes unless soil acidity is of concern. At present, our understanding of hydrochar surface chemistry and its interaction with nutrients, contaminants, and other soil organic matter is immature. Further research should focus

on developing production conditions and modification/activation methods that can produce hydrochars with characteristics tuned to meeting the needs of specific environmental applications.

Table 2-1. Properties of hydrochars produced from bagasse (B), hickory (H), and peanut hull (P) at 200 °C, 250 °C, and 300 °C.

Sample	Yield (%)	SA-N_2 (m^2/g)	PV-N_2 (cm^3/g)	SA-CO_2 (m^2/g)	PV-CO_2 (cm^3/g)	pH	Zeta potential (mv)
B200	47.75	10.7	0.215	106.3	0.034	4.0	-24.43
B250	33.50	3.9	0.035	93.2	0.030	5.3	-35.27
B300	26.75	4.9	0.034	86.8	0.027	5.8	-21.79
H200	54.60	7.8	0.121	137.2	0.043	4.9	-25.91
H250	49.60	8.9	0.110	121.6	0.038	5.1	-27.97
H300	27.80	1.8	0.008	120.0	0.037	5.4	-26.04
P200	50.55	7.1	0.010	100.1	0.032	6.2	-29.51
P250	44.91	1.1	0.010	56.3	0.019	6.2	-23.23
P300	36.91	UD	UD	64.7	0.023	6.0	-34.49

UD: Under detection limit, SA = surface area, and PV = pore volume.

Table 2-2. Bulk composition of hydrochars.

Sample	C%	H%	N%	O%	K%	Na%	Ca%	Mg%	S%	Fe%	P%	Al%	O:C	H:C	C:N
B200	69.15	5.11	0.54	25.74	0.01	0.03	0.03	0.02	0.05	0.01	0.00	0.01	0.37	0.07	128.06
B250	75.08	5.64	0.76	19.28	0.01	0.03	0.04	0.03	0.08	0.01	0.02	0.01	0.26	0.08	98.79
B300	79.31	5.34	0.88	15.35	0.01	0.04	0.06	0.03	0.11	0.01	0.03	0.01	0.19	0.07	90.64
H200	68.66	5.31	0.18	26.03	0.01	0.02	0.08	0.03	0.05	0.01	0.00	0.01	0.38	0.08	392.34
H250	70.00	5.02	0.54	24.98	0.01	0.04	0.07	0.04	0.09	0.03	0.00	0.01	0.36	0.07	129.63
H300	78.465	5.14	0.33	16.39	0.01	0.01	0.13	0.01	0.06	0.04	0.01	0.01	0.21	0.07	241.43
P200	70.575	6.04	1.86	23.39	0.03	0.02	0.07	0.02	0.14	0.04	0.06	0.01	0.33	0.09	38.05
P250	74.745	6.14	1.83	19.11	0.03	0.03	0.08	0.03	0.15	0.02	0.07	0.04	0.26	0.08	40.84
P300	76.415	6.07	2.06	17.52	0.03	0.02	0.16	0.05	0.13	0.03	0.17	0.04	0.23	0.08	37.09

Table 2-3. Elemental composition of the processing liquid (mg/L).

Sample	K	Na	Ca	Mg	S	Fe	Mn	Mo	Cu	P	Al	B
B200	172.9	10.9	157.2	74.8	142.8	57.3	1.7	0.4	1.7	11.0	1.5	0.8
B250	175.1	11.9	157.5	71.7	100.4	8.4	1.8	0.4	1.7	9.4	1.6	0.8
B300	164.9	10.9	149.8	40.5	89.2	UD	1.8	0.3	1.7	6.7	1.5	0.8
H200	181.3	6.8	186.7	108.2	49.6	0.5	16.7	0.4	1.7	6.8	1.7	0.9
H250	137.8	7.2	110.9	68.6	69.6	105.4	8.5	0.3	1.7	10.9	1.7	0.9
H300	174.0	6.1	138.4	107.0	65.8	60.1	16.2	0.3	1.7	1.7	1.7	1.0
P200	1013.6	8.3	86.7	116.4	319.0	32.5	5.0	0.4	1.7	33.1	1.7	1.0
P250	1079.2	12.1	81.5	124.3	362.6	0.5	4.6	0.4	1.7	45.6	1.6	0.7
P300	1036.8	10.5	40.5	99.0	327.4	0.0	2.5	0.3	1.7	7.4	1.5	0.7

UD: Under detection limit

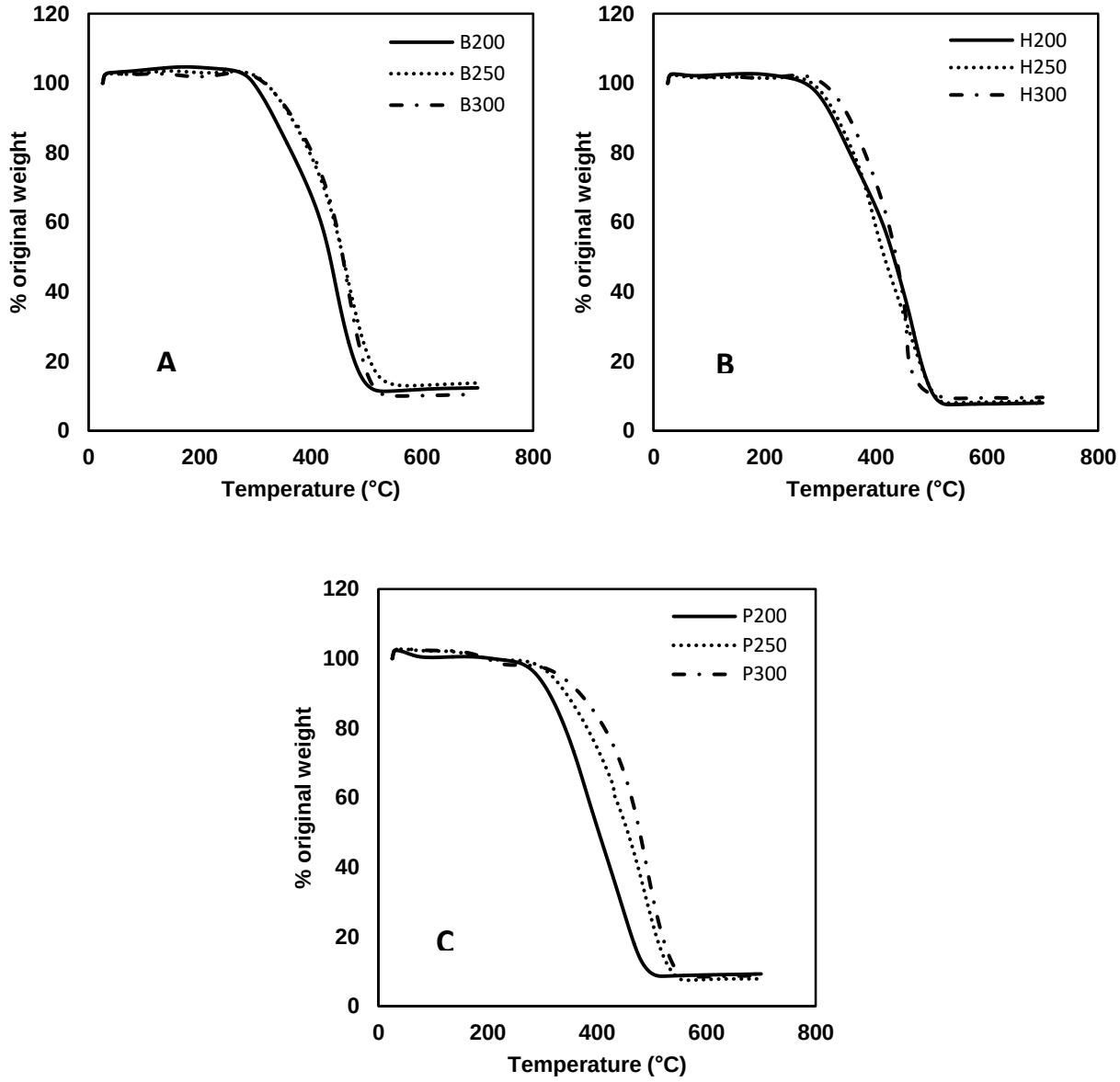

Figure 2-1. TGA curves of hydrochar. A) bagasse, B) hickory, and C) peanut hull

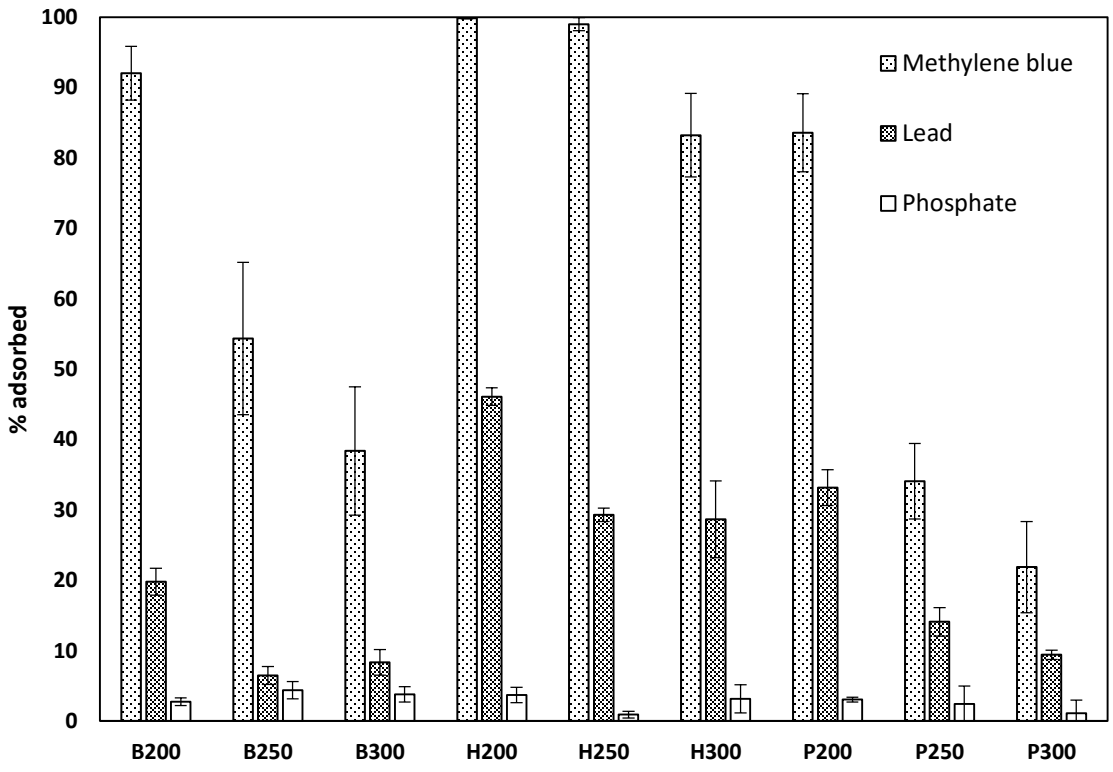

Figure 2-2. Hydrochar sorption of methylene blue, lead, and phosphate in aqueous solution.

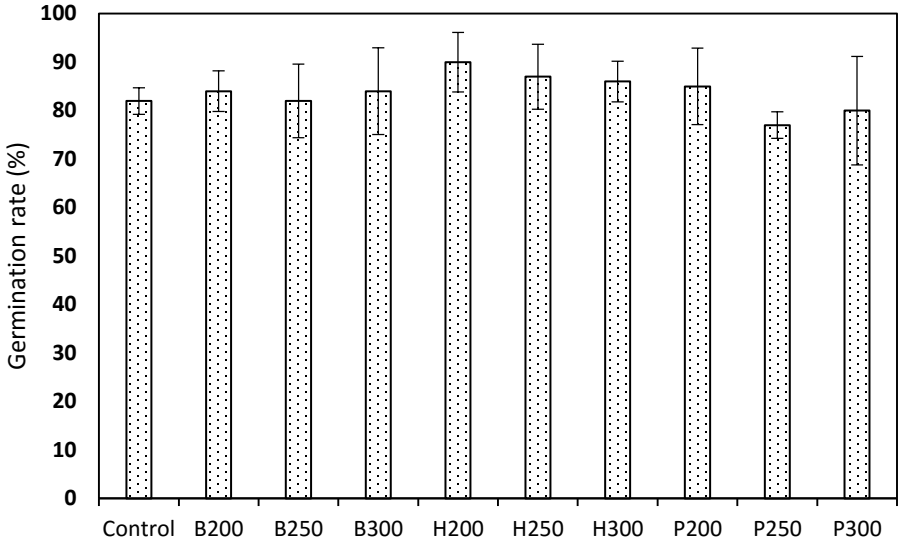

Figure 2-3. Effects of hydrochars on seed germination.

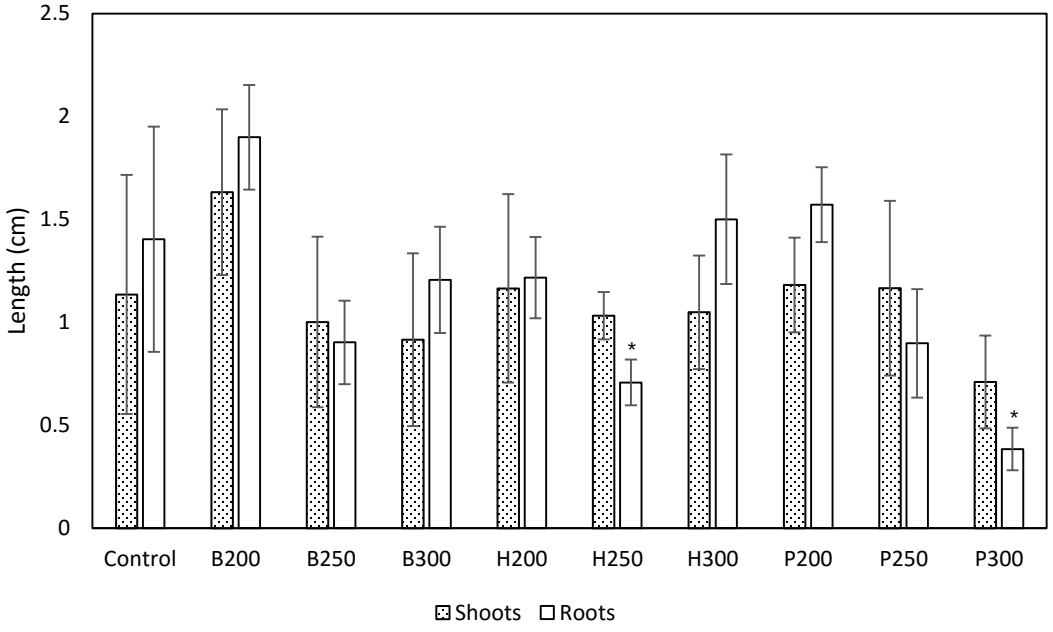

Figure 2-4. Effects of hydrochars on seedling growth.

CHAPTER 3
PHYSICALLY (CO_2) ACTIVATED HYDROCHARS FROM HICKORY AND PEANUT HULL: PREPARATION, CHARACTERIZATION, AND SORPTION OF METHYLENE BLUE, LEAD, COPPER, AND CADMIUM

Introduction

Hydrothermal carbonization (HTC) has attracted recent attention as a technique to convert biomass to useful carbonaceous products, due to several advantages it has over dry pyrolysis. Among these is its greater energy efficiency, because of higher yields of solids without need for energy-intensive drying compared to dry pyrolysis (Libra et al., 2011). Hydrochar, the resulting solid carbonaceous product from HTC (Libra et al., 2011), may be used for many of the same purposes as its dry pyrolysis counterpart, biochar, such as contaminant adsorption from soil and water, fuel, waste processing, and as a soil amendment for the purposes of carbon sequestration and fertility enhancement (Kammann et al., 2012; Lu et al., 2012; Ro et al., 2016; Sun et al., 2011; Xue et al., 2012). However, compared to biochar produced by dry pyrolysis, hydrochars generally have lower surface areas and pore volumes and higher volatile organic matter content, which are generally less desirable characteristics for most applications, particularly contaminant adsorption (Becker et al., 2013; Fang et al., 2015).

Activation, which commonly increases surface area and pore volume of pyrogenic biochar (Angin et al., 2013), might also improve the characteristics of hydrochar. Hydrochars often have high VOC contents that may not be removed through washing (Bargmann et al., 2013; Buss & Masek, 2014). An additional benefit of activation may be the removal of volatile matter through evaporation during heating. In addition, the low ash content of hydrochar makes it a more attractive option for activation than char created through dry pyrolysis. This is because the presence of

minerals may hinder pore and surface area development during the charring and activation processes (Ahmedna et al., 2000; Chang et al., 2000).

Activated carbons can be produced either through physical or chemical activation. Physical activation is similar to gasification with an oxidizing agent, commonly CO_2 or steam, at relatively high temperatures, typically between 600 and 1200 °C (Suhas et al., 2007). In contrast, chemical activation uses acids, bases, or salts to change the properties of a material's surface (Chang et al., 2000; Suhas et al., 2007). While coconut shells are often used in commercial production of activated carbon because of its low ash content, activated carbonaceous materials from a variety of alternative feedstocks, such as eucalyptus, coir pith, palm stones, and corn cobs, have been shown to be highly effective in the removal of contaminants such as dyes and heavy metals (Guo & Lua, 1998; Namasivayam & Kavitha, 2002; Ngernyen et al., 2006; Zhang et al., 2004).

While several studies have examined the sorptive properties of hydrochar and activated hydrochars (AHCs) for various contaminants (Hao et al., 2014; Mestre et al., 2015), few have examined the effects of activation conditions on AHC physicochemical properties and its resulting sorption ability. Thus, the objectives of this study were to investigate the effects of activation time and temperature during physical activation using CO_2 on the physicochemical characteristics of hickory and peanut hull hydrochars. The AHCs were tested for their ability to sorb a variety of contaminants (methylene blue, lead, copper, and cadmium) from aqueous solutions in batch reactions. Finally, the relationships between the AHC physicochemical properties and their sorption characteristics were examined in order to identify predominant sorption mechanisms.

Materials and Methods

Hydrochar Production and Activation

Hickory and peanut hull hydrochars were produced using the same procedure previously described (Fang et al., 2015). Briefly, feedstocks were milled to particle sizes of 0.5–1 mm and added to a pressurizable lidded stainless steel pot to a height of about one inch from the top (50 g of hickory and 55 g of peanut hull). Deionized (DI) water was added to the same level (290 and 313 mL of water, respectively). The pots were then sealed and heated on a hotplate to 200 °C for six hours (the HTC conditions to produce hydrochar with the highest yield and surface area) (Fang et al., 2015). The resulting hydrochars were rinsed for one hour by submersion in tap water and ten minutes in DI water to remove water soluble volatile matter, and oven dried for 24 hours at 70 °C. For activation, 5.0 g of the hydrochar were heated in a quartz tube furnace for either 1 or 2 hours, and at temperatures of 600, 700, 800 and 900 °C under CO_2 gas flowing at a rate of 150 mL min^{-1}. The AHCs were then allowed to cool to room temperature and were stored in an airtight container prior to characterization. The percentage of feedstock mass loss due to activation (burn-off degree) was calculated as:

$$\text{Burn-off degree (\%)} = \frac{W_0 - W}{W_0} \times 100\%$$

where W_0 is the original mass of hydrochar and W is the mass yield of activated hydrochar.

Activated Hydrochar Characterization

A CHN Elemental Analyzer (Carlo-Erba NA-1500) was used to determine the total carbon, hydrogen, and nitrogen contents of the activated hydrochars. Samples

were analyzed in duplicate and the averages are reported here. The surface areas (SA) of the samples were measured by N_2 sorptometry on a Quantachrome Autosorb I at 77 K and using the Brunauer–Emmett–Teller (BET) method in the 0.01 to 0.3 relative pressure range of the N_2 adsorption isotherm. Pore volumes (PV) were calculated from the desorption branch N_2 isotherms using Barrett–Joyner–Halenda (BJH) theory. Samples were de-gassed under vacuum at least 24 h at 180 °C prior to analysis.

Batch Sorption Experiments

Batch aqueous contaminant sorption experiments were carried out in triplicate at concentrations previously determined to be in the upper ends of their sorption ranges: methylene blue (700 ppm), lead (500 ppm), copper (20 ppm) and cadmium (20 ppm). All chemicals used were analytical grade and obtained from Fisher Scientific Co. and solutions were prepared using DI water (Nanopure water, Barnstead). Mixtures of 30 mL of each solution and 0.1 g of AHC in 68 mL digestion vessels were agitated on a mechanical shaker at 40 rpm for 24 hours. The solutions were then immediately filtered through 0.45 μm filter paper (Whatman). Aqueous lead, copper, and cadmium concentrations were analyzed using inductively coupled plasma spectroscopy (ICP-AES, Perkin Elmer Optima 2100 DV), and methylene blue was measured with a UV spectrometer (Thermo Scientific EVO 60) at a wavelength of 665 nm. The sorption rates of the AHCs were calculated as the difference between starting and final sorbate solution concentrations relative to the amount of sorbent (mmol kg^{-1}). One-way ANOVA tests were conducted using Minitab software to determine the statistical significance of the difference between each AHC's sorption ability and its nonactivated hydrochar counterpart.

Results and Discussion

Physicochemical Characteristics

Burn-off degree was generally greater for AHCs made from hickory versus peanut hull, varying from 50–72% and from 42–66%, respectively (Table 3-1). After activation, the hydrochars turned from dark brown to black, but no differences in color were observed between the different activation conditions. The differences in burn-off degree can partly be attributed to the structural composition of the two feedstocks. Peanut hull has a lignin content of 28%, compared to 18% for hickory (Guler et al., 2008; Maga, 1986). Feedstocks with high lignin content yield more solids when carbonized, while the holocellulosic fraction is more volatile (Suhas et al., 2007). Burn-off degree was generally similar for hydrochars activated at 600 and 700 °C for both activation times of 1 and 2 h, but increased when activated at 800 °C for 2 hours and at 900 °C for both 1 and 2 hours. These values are comparable to those found for other activated carbon materials. For example, activated carbons produced from oak, corn hulls, corn stover, eucalyptus, and wattle leaves had burn-off rates of 31.8–51.4% at 700–800 °C, 32.3–45.2% at 700–800 °C, 41.5–50.2% at 700–800 °C, 20.6–83% at 600–900 °C, and 21–67.1% at 600–900 °C, respectively (Lua et al., 2004; Ngernyen et al., 2006; Zhang et al., 2004).

Hickory and peanut hull AHC surface areas varied from 441–928 $m^2\ g^{-1}$ and from 309–1308 $m^2\ g^{-1}$, respectively. Burn-off degree was strongly correlated with surface area (R^2 = 0.86 and 0.76 for hickory and peanut hull, respectively). The two parameters generally increased with an increased activation temperature or time (Figure 3-1). As to the burn-off degree, SA increased most dramatically with an additional hour of treatment at 800 or 900 °C or with the temperature step increase from 800 to 900 °C. Pore

volume, however, did not show a clear relationship with activation time or temperature, but was greater for all AHC made from peanut hull. Interestingly, activation dramatically increased the surface area of hickory hydrochar but decreased the pore volume almost three times, on average. The decrease in pore volume could be attributed to the fact that at higher activation temperatures and longer activation times, the walls between pores could be destroyed, causing adjacent pores to fuse and create ones with larger diameters (Zhang et al., 2004). Sometimes, a sintering effect is created, where the pore walls collapse and decrease surface area due to the filling in of the pores (Guo & Lua, 1998). Other times, however, the destruction of walls increases the size of the pores and decreases microporosity, but total pore volume and surface area still increase. Thus, microporosity increases with increasing temperature and activation time, but after a certain point, pore diameters begins to increase and may or may not be accompanied by an increase in surface area. These patterns show that physical activation by CO_2 gasification has varying effects depending on biomass types. Apparently, removal of volatiles during activation increased the number of very small pores in the case of hickory hydrochar, while larger pores were opened during activation of peanut hull hydrochar. These volatiles of both hydrochars may be relatively H-rich and C-poor, as the C content increased and the H content decreased significantly following activation (Table 3-1).

Hydrochar Batch Sorption

Sorption of methylene blue (MB), lead (Pb), copper (Cu), and cadmium (Cd) by the AHCs ranged from 109.5–597.8, 36–225.4, 17.4–72.3, and 1.1–17.9 mmol kg^{-1}, respectively (Figure 3-2). While all the tested samples removed the contaminants from the solutions, the AHCs generally adsorbed more than the non-activated hydrochars.

Previous studies have shown that the surfaces of the two non-activated hydrochars are negatively charges (with zeta potential values of −25.91 and −29.51 mV, respectively) (Fang et al., 2015), enabling them to adsorb the cationic MB and heavy metals through electrostatic attractions. Further, the CO_2 activation process can introduce acidic functional groups to carbon surfaces (Wang et al., 2005), which might make the surfaces of the AHCs more negatively charged to promote the electrostatic attractions.

ANOVA tests showed that all of the AHCs sorbed significantly more methylene blue and lead than their respective non-activated hydrochars ($p < 0.05$). For hickory AHCs activated for 2 h at 600 °C, 1 h at 700 °C, and 1 h at 800 °C and peanut hull AHCs activated at 600 °C, sorption of copper did not differ from their non-activated hydrochars. Hickory AHCs sorbed significantly more Cd only when activated for 2 h at 800 °C and for 1 or 2 h at 900 °C, and peanut hull AHCs only when activated for 2 h at 700 °C and for 1 or 2 h at 800 °C and 900 °C.

The methylene blue and lead sorption rates of all of the AHCs in this work were below those maximum capacities of the commercial activated carbons (which range from 656.6–931.7 and 231.7–395.8 mmol kg^{-1} for methylene blue and lead, respectively (Aroua et al., 2008; Inyang et al., 2011; Kannan & Sundaram, 2001; Kumar et al., 2006)), however, the sorption rates of the AHCs made at 900 °C were only slightly lower. Because the sorption rates obtained in this work were obtained only at one initial sorbate concentration, they might be much lower than the maximum capacities obtained from the sorption isotherms. The sorption properties of the AHCs, particularly the ones activated at 900 °C, thus were comparable to that of the commercial activated carbons.

The sorption rates for all of the sorbates were positively correlated to AHC surface area (Figure 3-3) and the relationship was strongest for methylene blue and lead. This result indicates that the mechanism of interaction was via site specific interactions, i.e. surface adsorption. The amount of methylene blue sorbed by the AHC increased most when the activating temperature was increased to 900 °C (Figure 3-2 a). And although hickory AHCs showed a higher adsorption rate than the corresponding peanut hull activated at lower temperatures peanut hull AHC sorbed more methylene blue when produced at 900 °C. This pattern corresponds to the pattern or surface area for these AHCs (Table 3-1). Other studies have found the surface area of activated carbons to be correlated with adsorption rate of methylene blue. For example, activated carbon produced from olive waste cakes and *Posidonia oceanica* (L.) leaves adsorbed more methylene blue when activation conditions were adjusted to increase surface area (Bacaoui et al., 2001; Dural et al., 2011). The lignin contents of peanut hull and hickory also likely play a role. Lignin is usually the component that contributes to microporosity, and with peanut hull having higher amounts of lignin, the number of micropores would also be lower (Suhas et al., 2007). Thus, more methylene blue is adsorbed by hickory, which has less lignin and consequently has more pores with larger diameters than peanut hull. Methylene blue is a large molecule that would not be able to be fit into the smaller micropores on the surface of the AHCs.

Hickory AHCs sorbed more lead than peanut hull AHCs for all activation conditions (Figure 3-3 b), and the increases in sorption rate at 900 °C were not as large as they were for methylene blue. For peanut hull, the sorption rates of copper increased gradually with activation conditions, despite the dramatic increase in surface area at 900

°C. In addition, peanut hull oftentimes sorbed more copper at activation temperatures less than 900 °C. Weaker trends in cadmium sorption patterns with surface area were also observed for AHC made from both feedstocks (Figure 3-3 d). These weaker correlations between AHC surface area and copper and cadmium sorption suggest that these metals did not bind at all the available AHC binding sites. The size of the hydrated ionic radii of the metals likely explains the differences in their ability to be sorbed by the AHCs, where sorption rate is inversely correlated with hydrated ionic radii. The hydrated ionic radii of the metals follow the order Cd^{2+} (4.26 Å) > Cu^{2+} (4.19 Å) > Pb^{2+} (4.01 Å). As the hydrated ionic radius increases, the ion becomes more distant from the surface it is to be adsorbed onto. Thus, the sorption ability is stronger for ions with a smaller hydrated ionic radii (Chen et al., 2010).

AHC pore volume was not correlated with sorption rates for any of the contaminants, further suggesting that sorption occurred by a surface site-related, rather than pore-filling mechanism (Figure 3-4). Mixed results in the relationship between pore volume and sorption rates have been observed; while methylene blue sorption increased with pore volume of activated carbons made from *Posidonia oceanica* (L.) leaves, there was no such relationship for activated carbons made from coal or coconut shells (Dural et al., 2011; Wang et al., 2005).

Conclusions

CO_2 activation of hydrochar resulted in an increase in surface area, which led to greater sorption of methylene blue and lead at all activation temperatures, but cadmium and copper sorption increased only at activation temperatures of 700–900 °C. In general, the higher the temperature and the longer the activation time, the greater the

AHC ability to adsorb a range of contaminant from aqueous solution. Because hydrothermal carbonization is more energy efficient than dry pyrolysis, the use of AHCs may prove to be a more cost-effective and environmentally friendly alternative to traditional activated carbons for environmental applications.

Table 3-1. Bulk properties of activated hickory and peanut hull hydrochars.

Feedstock	Activation Temperature (C)	Activation time (h)	Burn-off (%)	BET-SA (m^2 g^{-1})	BJH-PV (mL g^{-1})	C (wgt. %)	H (wgt. %)	N (wgt. %)
Hickory	nonactivated	-	-	8	0.121	68.7	5.3	0.2
	600	1	50	445	0.038	85.1	2.8	0.2
	600	2	52	453	0.050	88.1	2.8	0.2
	700	1	54	441	0.044	90.1	1.6	0.2
	700	2	54	465	0.049	90.3	0.6	0.3
	800	1	56	474	0.040	91.0	0.4	0.3
	800	2	70	667	0.041	89.1	0.4	0.3
	900	1	66	703	0.053	90.6	0.7	0.4
	900	2	72	928	0.054	90.5	0.2	0.4
Peanut hull	nonactivated	-	-	7	0.010	70.6	6.0	1.9
	600	1	46	310	0.079	70.6	6.0	1.9
	600	2	48	353	0.075	84.8	2.0	2.3
	700	1	48	349	0.067	86.5	2.2	2.3
	700	2	46	365	0.114	88.7	1.5	2.3
	800	1	48	345	0.056	87.7	1.4	2.2
	800	2	58	488	0.069	87.7	1.2	2.3
	900	1	66	988	0.121	86.6	2.0	2.6
	900	2	62	1308	0.114	86.5	2.9	2.2

SA = surface area and PV = pore volume

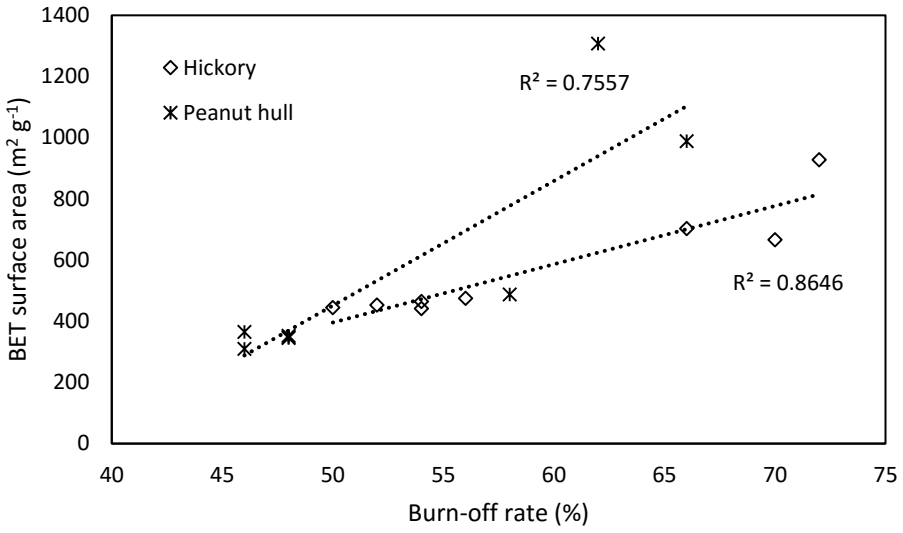

Figure 3-1. Relationship between hydrochar burn-off degree and surface area.

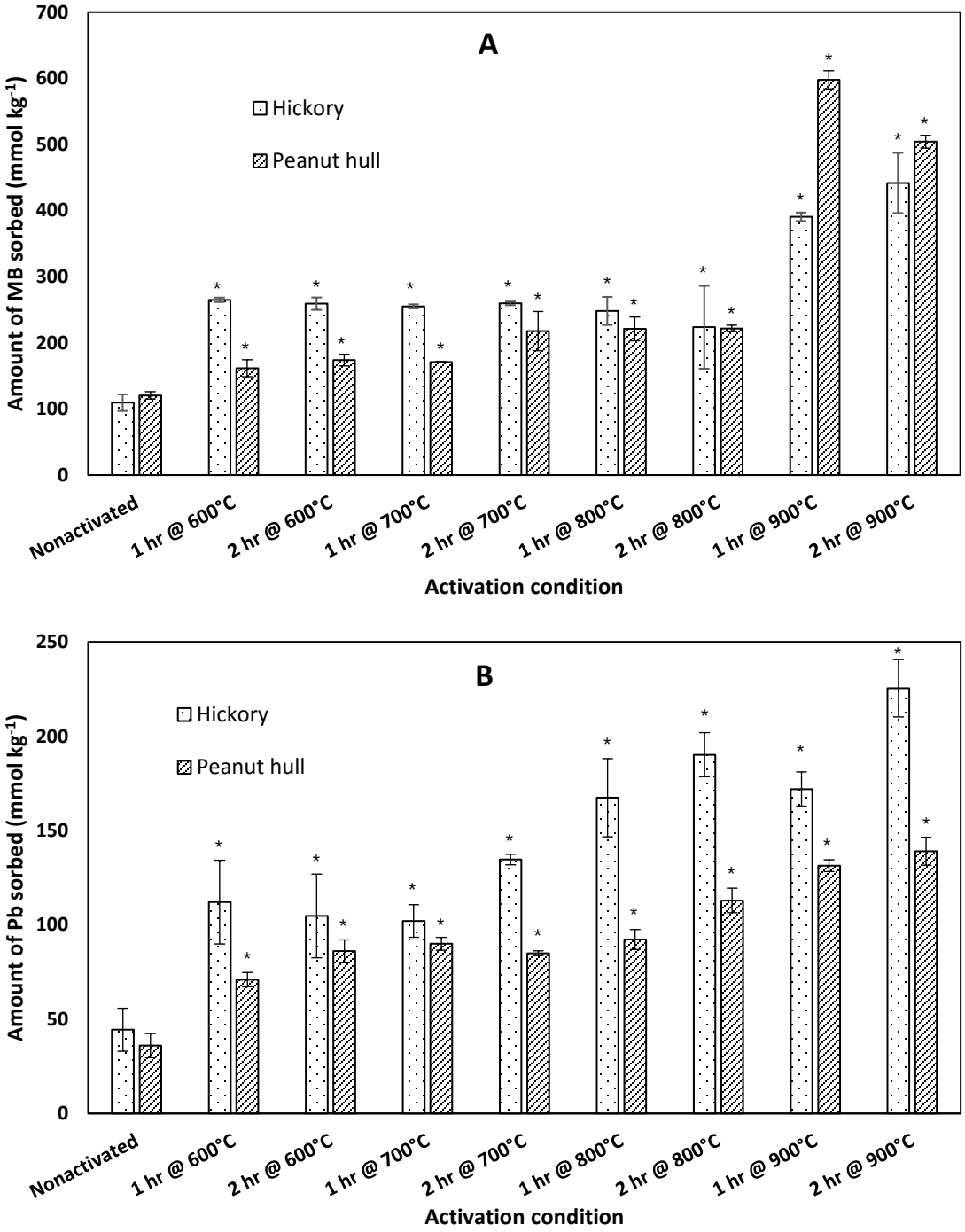

Figure 3-2. Removal of contaminants by AHCs from aqueous solution. A) Methylene blue, B) Pb, C) Cu, and D) Cd

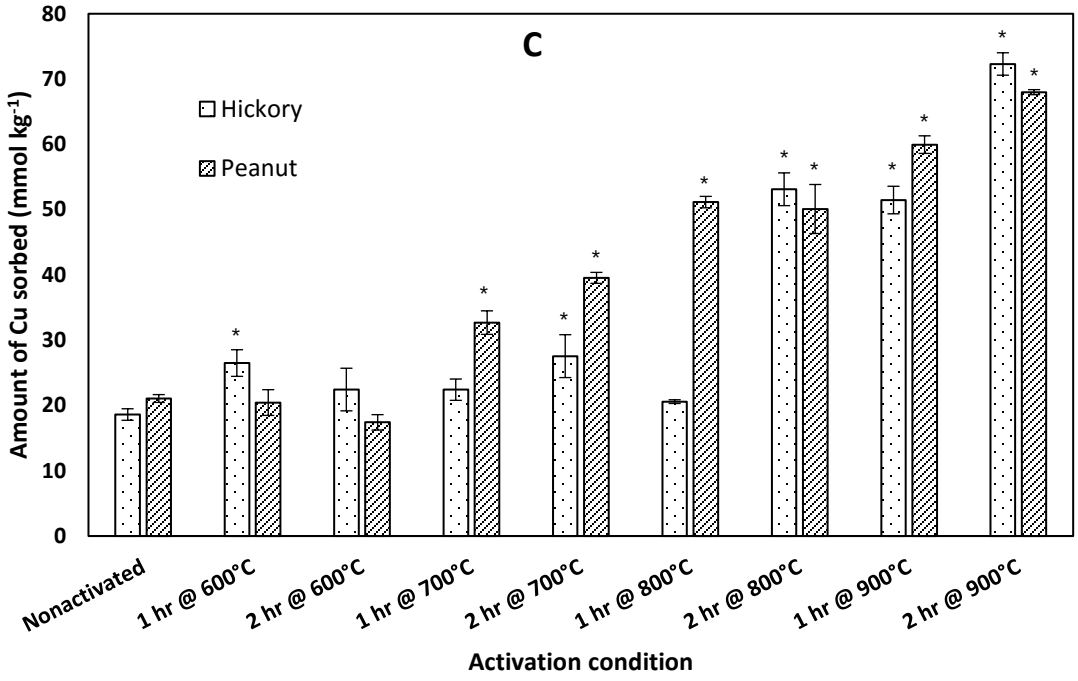

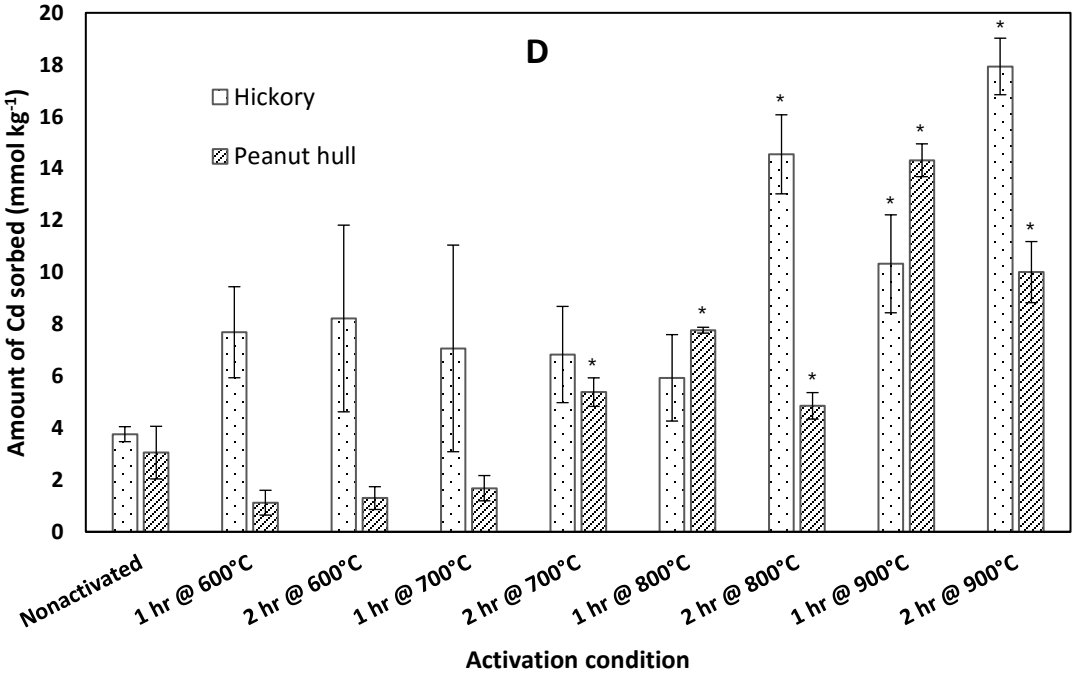

Figure 3-2. Continued

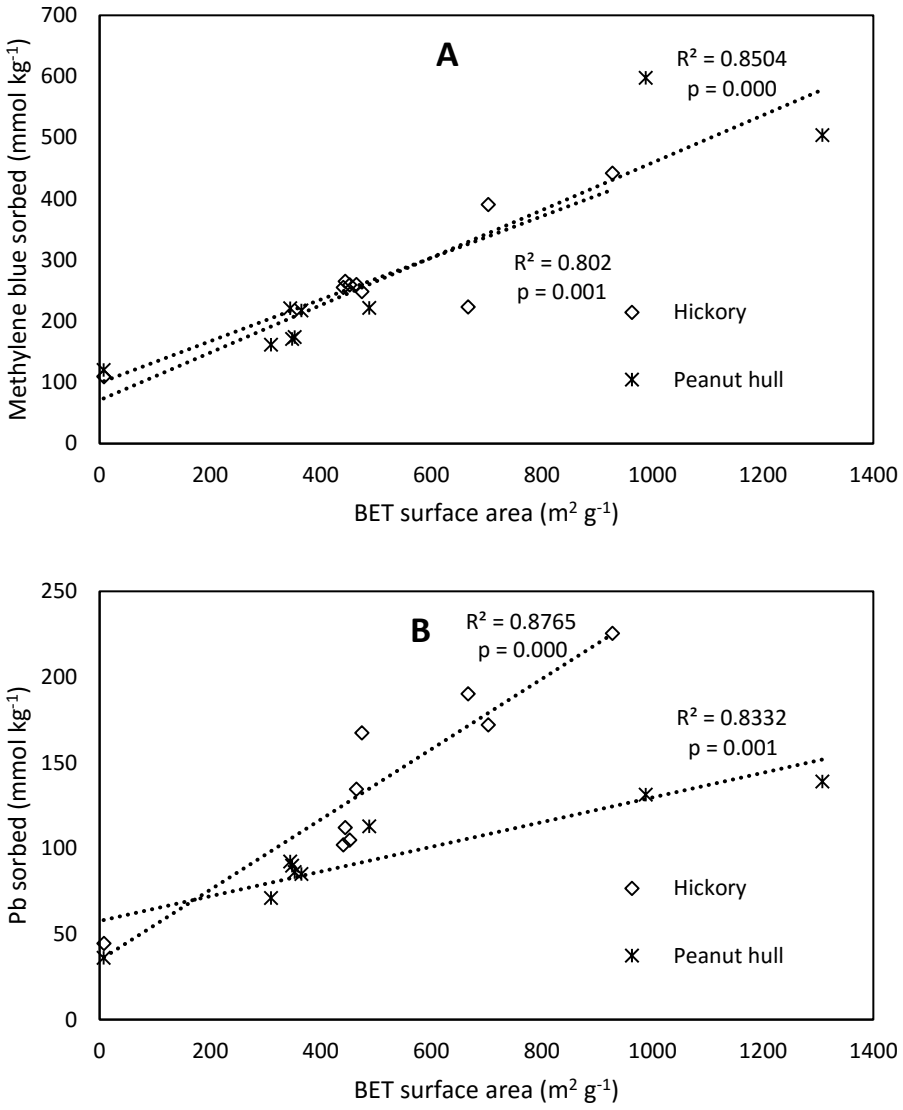

Figure 3-3. Relationship between surface area and amount of contaminant sorbed by AHCs. A) Methylene blue, B) Pb, C) Cu, and D) Cd

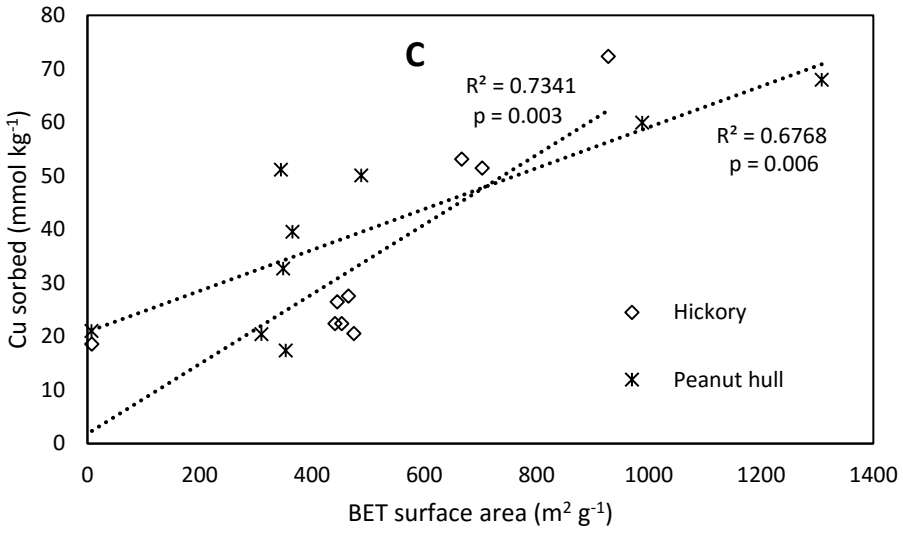

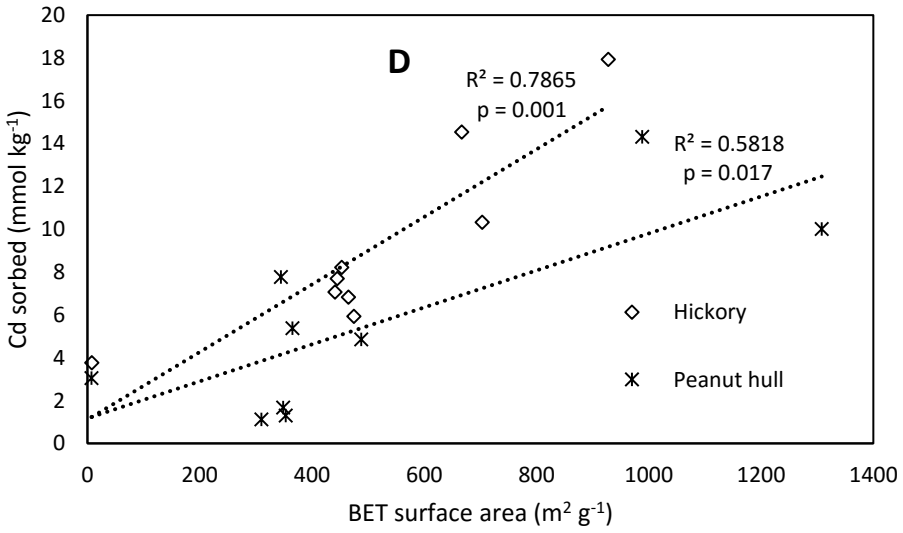

Figure 3-3. Continued

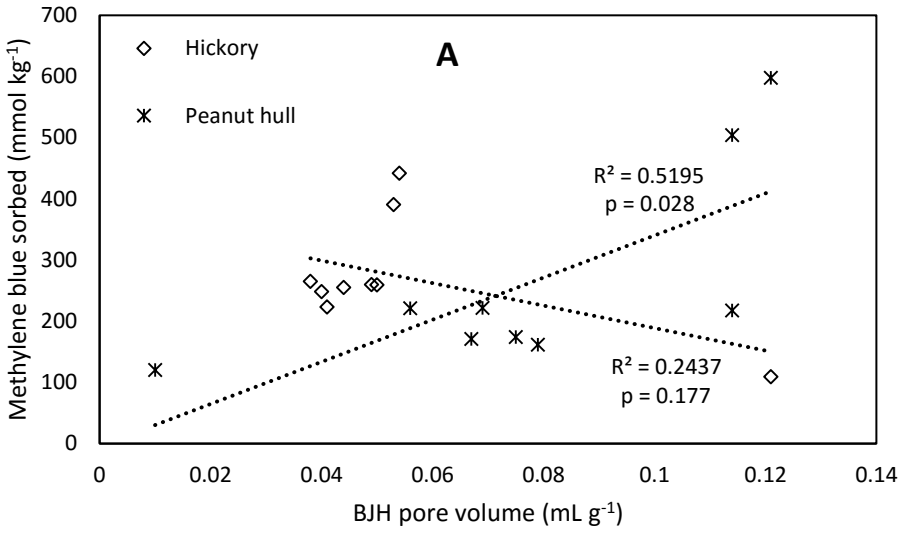

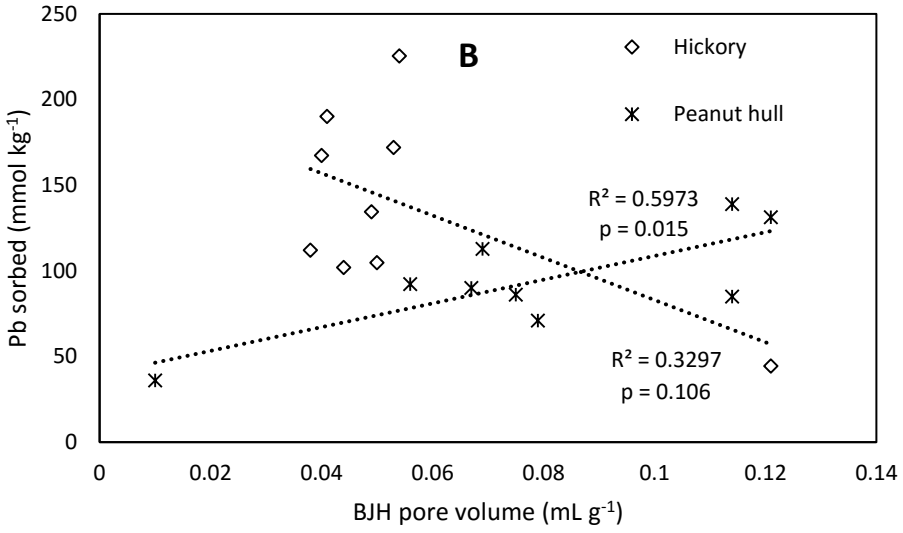

Figure 3-4. Relationship between pore volume and amount of contaminant sorbed by AHCs. A) Methylene blue, B) Pb, C) Cu, and D) Cd

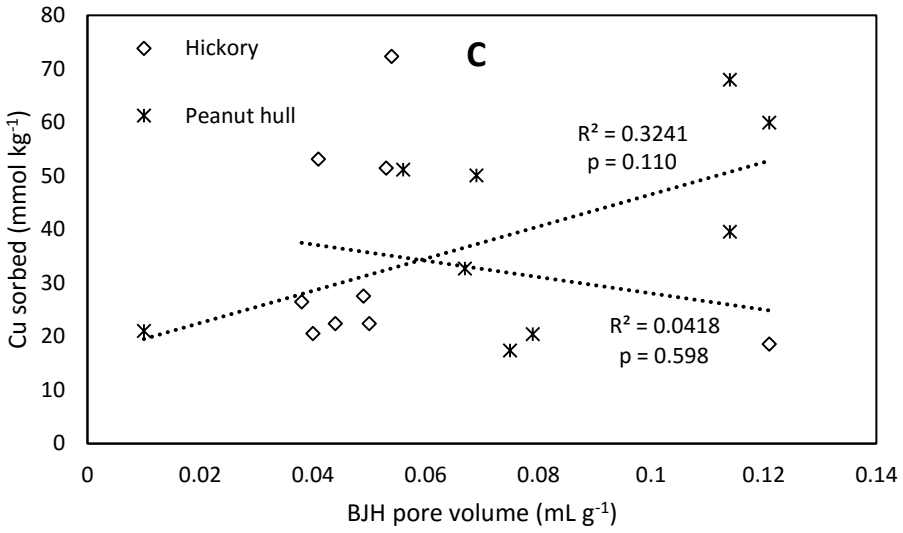

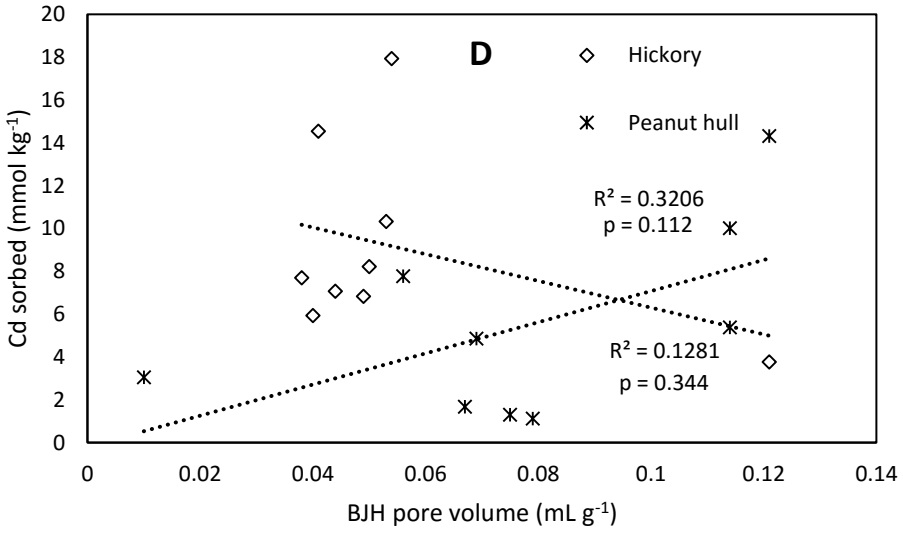

Figure 3-4. Continued

CHAPTER 4
CHEMICAL ACTIVATION OF HICKORY AND PEANUT HULL HYDROCHARS FOR REMOVAL OF LEAD AND METHYLENE BLUE FROM AQUEOUS SOLUTIONS

Introduction

There are needs for carbon based adsorbents, particularly activated carbon (AC), for the removal of aqueous contaminants. Water bodies are often contaminated due to discharges by industrial activity, and it is a major concern throughout the world due to the ecological and health risks it poses (Inyang et al., 2012). AC may be produced from any organic feedstock, but it is usually commercially produced from coconut shells and coal (Girgis et al., 2002). Since there is an abundance of agricultural and industrial wastes produced throughout the world, many studies have explored the processing of these waste materials into AC as a low cost alternative to commercial AC. Some of the feedstocks tested include waste tires, coir pith, bagasse, olive mill waste, corn cobs, and apricot stones (Bacaoui et al., 2001; Betancur et al., 2009; Chang et al., 2000; Kobya et al., 2005; Namasivayam & Kavitha, 2002; Valix et al., 2004). These feedstocks have been found to produce ACs that are highly effective for the removal of dyes and heavy metals.

In order to obtain the best properties for adsorption, the feedstock used must have a low ash content, as the presence of inorganic elements weakens the structure of the AC, causing pore collapse in the carbon matrix (Ahmadpour & Do, 1996). When coals are used as feedstocks for AC, it has been found that the higher the rank of the coal, the more resistant it is to activation, whether physical or chemical (Lillo-Rodenas et al., 2004). Lignite would thus be a better choice for AC production than anthracite. However, lignite has drawbacks including a high ash content and a high sulfur content, which is also considered a water contaminant (Jia et al., 2016). Hydrochar, therefore,

could be considered as an alternative to lignite as feedstock to AC production. Its degree of coalification is similar to lignite, but it has a low ash and sulfur content. Hydrochar is also a poor adsorbent when used as is due to its low surface area and high volatiles content, and activation would help improve its properties (Fang et al., 2015; Sun et al., 2014).

While several studies have examined the sorptive properties of hydrochar for various contaminants, few have examined the effects of chemical activation on hydrochar's physicochemical properties and its ability to adsorb contaminants (Fernandez et al., 2015; Xue et al., 2012). Thus, the objectives of this study were to investigate the effects of H_3PO_4 and KOH chemical activation on the physicochemical characteristics of hickory and peanut hull hydrochars. H_3PO_4 and KOH were chosen because they have been well-established as highly effective activating agents and also so that the effects of both an acid and a base on the physicochemical characteristics of hydrochar can be investigated. The AHCs were tested for their ability to adsorb a variety of methylene blue and lead from aqueous solutions in batch reactions. Finally, the relationships between the AHC physicochemical properties and their sorption characteristics were examined in order to identify predominant sorption mechanisms.

Materials and Methods

Hydrochar Production and Activation

Hickory and peanut hull hydrochars were produced using the same procedure previously described (Fang et al., 2015). Briefly, feedstocks were milled to particle sizes of 0.5-1 mm and added to a pressurizable lidded stainless steel pot to a height of about one inch from the top (50 g of hickory and 55 g of peanut hull). Deionized (DI) water was added to the same level (290 and 313 mL of water, respectively). The pots were

then sealed and heated on a hotplate to 200 °C for six hours, which were the HTC conditions that produced hydrochar with the highest yield and surface area (Fang et al., 2015). The resulting hydrochars were rinsed for one hour by submersion in tap water and ten minutes in DI water to remove water soluble volatile matter, and oven dried for 24 hours at 70 °C. For activation, the hydrochar was mixed in a 1:1 w/w ratio with either KOH or 85% H_3PO_4 solution. The mixture was stirred on top of a hotplate for 2 hours at 85°C, and the resulting slurry was oven dried for 24 hours at 100 °C. The dried slurry was then activated in a tube furnace for 1 hr at 600 °C under N_2 gas flowing at a rate of 150 mL min^{-1}. The AHCs were then allowed to cool to room temperature, and were washed with DI water in order to remove any residual chemicals. They were rinsed repeatedly with DI water until the pH of the AHC-water mixture stabilized.

Activated Hydrochar Characterization

A CHN Elemental Analyzer (Carlo-Erba NA-1500) was used to determine the total carbon, hydrogen, and nitrogen contents of the activated hydrochars. Samples were analyzed in duplicate and the averages are reported here. The surface areas (SA) of the samples were measured by N_2 sorptometry on a Quantachrome Autosorb I at 77 K and using the Brunauer-Emmett-Teller (BET) method in the 0.01 to 0.3 relative pressure range of the N_2 adsorption isotherm. Pore volumes (PV) were calculated from the desorption branch N_2 isotherms using Barrett-Joyner-Halenda (BJH) theory. Samples were de-gassed under vacuum at least 24 h at 180 °C prior to analysis.

Batch Sorption Experiments

Batch aqueous contaminant sorption experiments were carried out in triplicate. All chemicals used were analytical grade and obtained from Fisher Scientific Co. and solutions were prepared using DI water (Nanopure water, Barnstead). Mixtures of 30

mL of each solution and 0.1 g of AHC in 68 mL digestion vessels were agitated on a mechanical shaker at 40 rpm. For sorption kinetics experiments, the AHCs were tested at 500 ppm for lead and 700 ppm for methylene blue, and samples were withdrawn at time intervals ranging from 0.5-24 hours. For sorption isotherm experiments, the AHCs were mixed with solutions ranging from 10-1000 ppm for methylene blue and 10-700 ppm for lead and then shaken for 24 hours. The solutions were then immediately filtered through 0.45 um filter paper (Whatman). Aqueous lead concentrations were analyzed using inductively coupled plasma spectroscopy (ICP-AES, Perkin Elmer Optima 2100 DV), and methylene blue was measured with a UV spectrometer (Thermo Scientific EVO 60) at a wavelength of 665 nm. The sorption rates of the AHCs were calculated as the difference between starting and final sorbate solution concentrations relative to the amount of sorbent (mg g^{-1}).

Mathematical Models

Pseudo-first-order, pseudo-second-order, and Elovich models were used to simulate the sorption kinetics data. Governing equations for these models can be written as (Inyang et al., 2012):

First-order: $q_t = q_e(1 - e^{-k_1 t})$,

Second-order: $q_t = \frac{k_2 q_e^2 t}{1+k_2 q_e^2 t}$,

Elovich: $q_t = \frac{1}{\beta}\ln(\alpha\beta t + 1)$,

where q_t and q_e are the amount of sorbate removed at time t and at equilibrium, respectively (mg g^{-1}); k_1 and k_2 are the first-order and second-order sorption rate constants (h^{-1}), respectively; α is the initial sorption rate (mg g^{-1}); and β is the

desorption constant (g mg^{-1}). The first- and second-order models are semi-empirical equations, while the Elovich model is an empirical fitting equation.

The Langmuir and Freundlich models were used to simulate the sorption isotherms. Their governing equations can be written as (Inyang et al., 2012):

Langmuir: $q_e = \frac{KS_{max}C_e}{1+KC_e}$,

Freundlich: $q_e = K_f C_e^n$,

where K and K_f are the Langmuir bonding term related to interaction energies (L mg^{-1}) and the Freundlich affinity coefficient ($mg^{(1-n)}$ L^n g^{-1}), respectively; S_{max} is the Langmuir maximum capacity (mg kg^{-1}); C_e is the equilibrium solution concentration (mg L^{-1}) of the sorbate; and n is the Freundlich linearity constant. The Langmuir model assumes monolayer adsorption onto a homogeneous surface with no interactions between the adsorbed molecules. The Freundlich model is an empirical equation commonly used for heterogeneous surfaces.

Results and Discussion

Physicochemical Characteristics

Chemical activation greatly increased the surface area of the hydrochars, especially with H_3PO_4. Hickory and peanut hull hydrochars activated with H_3PO_4 had surface areas of 1436 and 1091 m^2 g^{-1}, respectively. While hickory had a surface area almost 50% greater than that of peanut hull after undergoing H_3PO_4 activation, peanut hull had a surface area that was twice as large as hickory when KOH activation was used (571 vs. 222 m^2 g^{-1}). This suggested that hickory hydrochar might be a better feedstock for the production of high surface area ACs. In the hickory AHCs, pore volume decreased after activation despite the increase in surface area, although the

pore volume of peanut hull AHCs increased along with an increase in surface area (Table 4-1). The pore volumes of all of the chemically AHCs are lower than those of the physically AHCs (Table 4-1). Previous studies have shown that chemical activated AC may have relatively low pore volume due to the lower burn-off rate compared to physical activation (Salas-Enriquez et al., 2016).

Compared to physically AHCs, the chemically AHCs have a lower C content. In addition, the chemically AHCs also had slightly lower C content than the hydrochar they were synthesized from (Table 4-1). The chemical activation process produces oxygenated functional groups on the surface of the hydrochar as a result of the chemicals that are added, whereas in physical activation, less functional groups are formed and the proportion of C in the AHC increases (Xue et al., 2012). H_3PO_4 activation produced hickory hydrochar with a higher surface area than did physical activation, and although it increased surface area of the peanut hull hydrochar, it did not increase as much as it did with physical activation. This indicated that feedstock type was also an important factor in the differences between physicochemical characteristics of the AHCs.

Final yields of chemically AHCs ranged from 40-54% of the original weight of hydrochar used. These yields are comparable to those obtained with physical activation at 600-800 °C, but were higher than physically AHCs obtained at 900 °C. However, for both hickory and peanut hull, the surface areas of the H_3PO_4 AHCs were more similar to those of the 900 °C physically AHCs. KOH AHC from peanut hulls had a surface area that was in between those that were physically activated at 600-800 and 900 °C, while KOH AHC from hickory had a surface area than those at all physical activation

temperatures. The comparability in morphology between the chemically AHCs and the 900ºC physically AHCs despite differences in yield indicates that activation of hydrochar is more efficient with chemicals. This is because the addition of chemicals inhibits the formation of tars during activation. During physical activation, tars are formed and volatilized, increasing the amount of char that is burned off (Kandiyoti et al., 1984).

Batch Sorption Experiments

An initial assessment of the chemically AHCs were conducted that showed the chemically activated hydrochars were better able to sorb lead than raw and physically activated hydrochar, with sorption rates ranging from 95-162.3 mg Pb g^{-1}, compared to 9.2-46.7 mg Pb g^{-1} (Figure 4-1). The hickory AHCs had higher sorption rates than the peanut hull AHCs, and for both feedstocks, KOH created hydrochars with higher sorption rates than H_3PO_4. For methylene blue, chemically activated hydrochars had higher sorption rates than their raw counterparts, but were lower than that of their physically activated counterparts. The only exception to this is H_3PO_4 activated hickory hydrochar, which has a sorption rate of 208.6 mg g^{-1} compared to 141.3 mg Pb g^{-1} for the physically activated hickory hydrochar. This is probably due to the much higher surface area of the H_3PO_4 hickory than those of the other AHCs.

Kinetics experiments showed that all of the AHCs were able to adsorb MB within 10 hours and lead within 5 hours (Figures 4-2 and 4-3). The quick kinetics of lead adsorption indicate that precipitation is one of the predominant mechanisms involved in the removal of lead from solution (Largitte et al., 2014). As shown in Tables 4-2 and 4-3, the Elovich model fits the data for lead sorption by H_3PO_4 peanut hull AHC and MB sorption by all of the AHCs (except H_3PO_4 hickory AHC), indicating that sorption in these instances involves chemisorption onto heterogeneous surfaces (Zhang & Gao,

2013). The second-order model fit the remaining data the best, suggesting sorption of MB and lead onto these AHCs follows the binuclear mechanism (Xue et al., 2012). For MB adsorption isotherms, the Langmuir model fit the H_3PO_4 AHCs better than the Freundlich model, while Freundlich was a better fit for the KOH AHCs than Langmuir (Table 4-3). For the adsorption of lead, Langmuir was a better fit than Freundlich for all of the AHCs, as indicated by their higher R^2 values (Table 4-2). The Langmuir model assumes monolayer adsorption on a homogeneous surface with no interaction between the adsorbed molecules, while the Freundlich model is used to describe chemisorption onto heterogeneous surfaces (Yao et al., 2011).

Sorption Mechanisms

Different mechanisms of sorption are likely at play with lead and MB, explaining why their rates of sorption are different according to the type of chemical used in activation. MB is a large organic molecule, while lead is smaller. KOH activation is known to produce highly microporous ACs, while H_3PO_4 has a higher proportion of meso- and macro- pores (Hui & Zaini, 2015). The MB is therefore unable to access many of the sorption sites on the KOH AHCs (Altenor et al., 2009; Hui & Zaini, 2015). Likewise, H_3PO_4 also produces more micropores than physical activation; as a result, physically AHCs have a higher capacity for MB than the chemically AHCs (Salas-Enriquez et al., 2016). The exception to this is H_3PO_4 hickory, since the higher surface area compensates for the lower proportion of micropores, and more meso- and macro-porous sorption sites are provided. Although the KOH AHCs had surface areas that were five times lower than that of the H_3PO_4 AHCs, they were able to adsorb more lead. This indicates that in addition to the number of available sorption sites, surface oxygenated functional groups play a large role in the removal of lead from solution, as

KOH tends to produce more functional groups than H_3PO_4. KOH activation of maize stalks have been found to produce ACs that are highly effective at removing Pb^{2+} from solution, and this was attributed to the micropores and functional groups that developed on the maize stalks after activation (El-Hendawy, 2009). The surface functional groups remove lead from solution precipitation, a mechanism that is confirmed by the quick adsorption kinetics of the AHCs and lead shown in Figure 4-3. Figure 4-6 shows the relationship between surface area and the amount of contaminant sorbed by raw and activated hydrochars. There is a higher correlation between sorption and surface area with MB (R^2 = 0.91) than there is with Pb (R^2 = 0.06), confirming that surface area predominantly governs MB sorption and surface chemistry of the sorbent more important in Pb sorption.

Conclusions

Chemical activation of hydrochar resulted in an increase in surface area, which led to greater sorption of methylene blue and lead compared to the original unmodified hydrochar and in the case of lead when compared to CO_2 physical AHCs. For methylene blue, the physical AHCs had higher adsorption capacities than the chemical AHCs, with the exception of H_3PO_4 hickory AHC. In general, the higher the temperature and the longer the activation time, the greater the AHC ability to adsorb a range of contaminant from aqueous solution. This could be linked to increases in surface area with activation time and temperature and suggests that surface adsorption was the governing mechanism. The AHCs produced at 900 °C sorbed methylene blue and lead at rates comparable to those of commercial activated carbons. Although these sorption rates are at the lower end of the range, further exploration of other hydrochar feedstock

materials and activation conditions would likely yield AHCs with even higher sorption efficiencies. Because hydrothermal carbonization is more energy efficient than dry pyrolysis, the use of AHCs may prove to be a more cost-effective and environmentally friendly alternative to traditional activated carbons for contaminant remediation and water treatment applications.

Table 4-1. Bulk properties of activated hickory and peanut hull hydrochars.

Feedstock	Activating chemical	Wgt. after activation (g)	Wgt. after washing (g)	Final yield (%)	BET-SA (m^2 g^{-1})	BJH-PV (mL g^{-1})	C (wgt. %)	N (wgt. %)
Hickory	nonactivated	-	-	-	8	0.121	68.7	0.2
	H_3PO_4	5.8	2	40	1436	0.028	62.8	0.2
	KOH	7.9	2.7	54	222	0.050	68.3	0.2
Peanut hull	nonactivated	-	-	-	7	0.010	70.6	1.9
	H_3PO_4	6.5	2.6	52	1091	0.079	41.5	1.1
	KOH	7.8	2.7	54	571	0.075	67.3	1.5

SA = surface area and PV = pore volume

Table 4-2. Best-fit model parameters of lead sorption on AHCs

		Parameter 1	Parameter 2	R^2
Hickory H_3PO_4	First-order	$k_1 = 4.178$	$q_e = 109.8$	0.574
	Second-order	$k_2 = 0.151$	$q_e = 111.0$	0.480
	Elovich	$\alpha = 2.7 \times 10^{16}$	$\beta = 0.610$	0.146
	Langmuir	$K = 0.074$	$S_{max} = 92.1$	0.927
	Freundlich	$K_f = 11.697$	$n = 0.346$	0.840
Hickory KOH	First-order	$k_1 = 0.921$	$q_e = 157.2$	0.939
	Second-order	$k_2 = 0.008$	$q_e = 169.1$	0.993
	Elovich	$\alpha = 1408$	$\beta = 0.042$	0.933
	Langmuir	$K = 0.022$	$S_{max} = 135.7$	0.997
	Freundlich	$K_f = 7.560$	$n = 0.494$	0.981
Peanut H_3PO_4	First-order	$k_1 = 2.325$	$q_e = 90.5$	0.833
	Second-order	$k_2 = 0.049$	$q_e = 94.0$	0.901
	Elovich	$\alpha = 4.9 \times 10^5$	$\beta = 0.148$	0.996
	Langmuir	$K = 0.032$	$S_{max} = 162.1$	0.996
	Freundlich	$K_f = 12.34$	$n = 0.473$	0.947
Peanut KOH	First-order	$k_1 = 1.459$	$q_e = 122.5$	0.676
	Second-order	$k_2 = 0.016$	$q_e = 131.2$	0.737
	Elovich	$\alpha = 3916$	$\beta = 0.063$	0.696
	Langmuir	$K = 0.026$	$S_{max} = 158$	0.957
	Freundlich	$K_f = 11.810$	$n = 0.458$	0.863

Table 4-3. Best-fit model parameters of methylene blue sorption on AHCs

		Parameter 1	Parameter 2	R^2
Hickory H_3PO_4	First-order	k_1 = 0.677	q_e = 195.8	0.888
	Second-order	k_2 = 0.004	q_e = 214.6	0.962
	Elovich	α = 660.553	β = 0.028	0.956
	Langmuir	K = 70.343	S_{max} = 187.3	0.822
	Freundlich	K_f = 134.004	n = 0.132	0.578
Hickory KOH	First-order	k_1 = 1.014	q_e = 51.9	0.721
	Second-order	k_2 = 0.023	q_e = 56.7	0.799
	Elovich	α = 325.760	β = 0.115	0.838
	Langmuir	K = 2.350	S_{max} = 49.8	0.870
	Freundlich	K_f = 23.798	n = 0.244	0.958
Peanut H_3PO_4	First-order	k_1 = 0.451	q_e = 142.5	0.936
	Second-order	k_2 = 0.003	q_e = 161.1	0.979
	Elovich	α = 196.470	β = 0.032	0.983
	Langmuir	K = 51.852	S_{max} = 135.5	0.920
	Freundlich	K_f = 93.080	n = 0.206	0.888
Peanut KOH	First-order	k_1 = 0.603	q_e = 48.8	0.683
	Second-order	k_2 = 0.013	q_e = 55.2	0.823
	Elovich	α = 97.433	β = 0.097	0.922
	Langmuir	K = 1.808	S_{max} = 49.9	0.869
	Freundlich	K_f = 23.290	n = 0.247	0.955

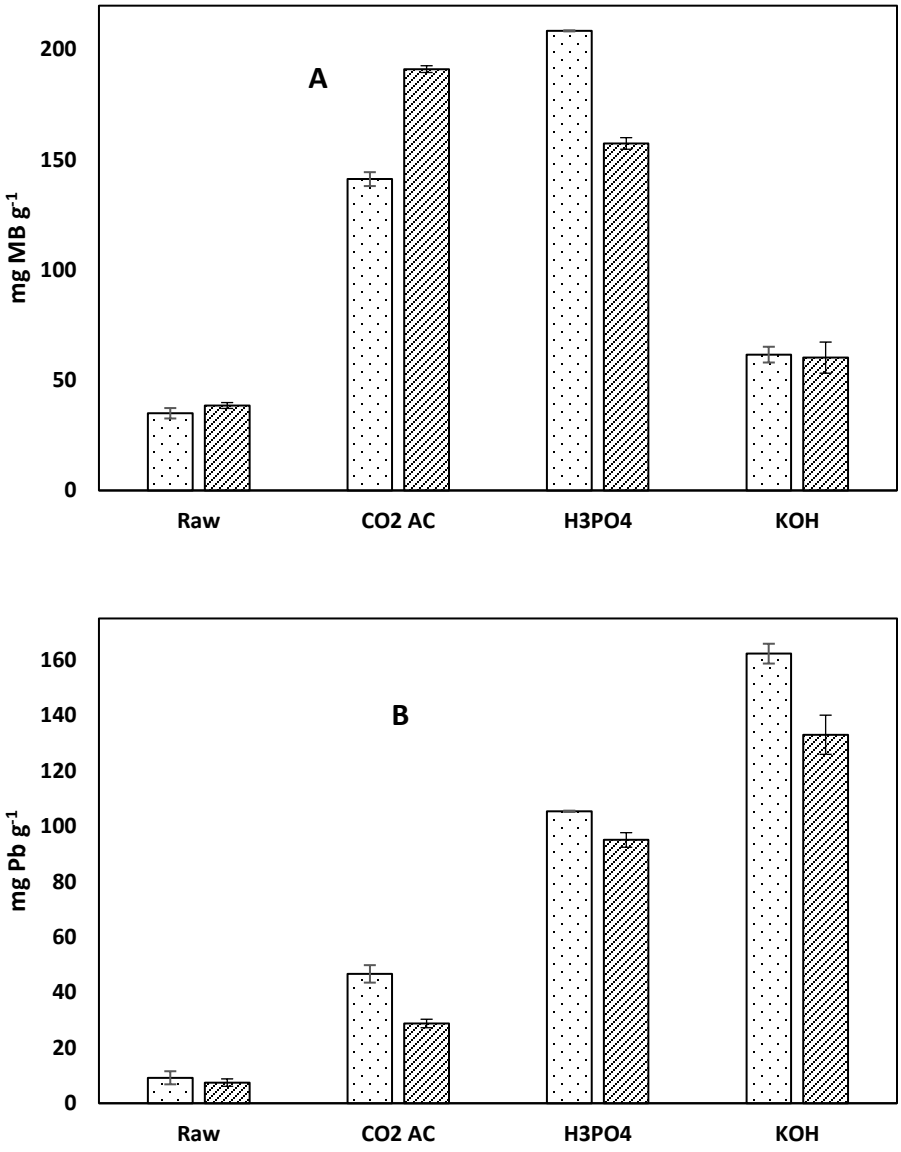

Figure 4-1. Comparison of chemically AHC with physically AHC and raw hydrochar for the sorption of contaminants. A) methylene blue and B) lead

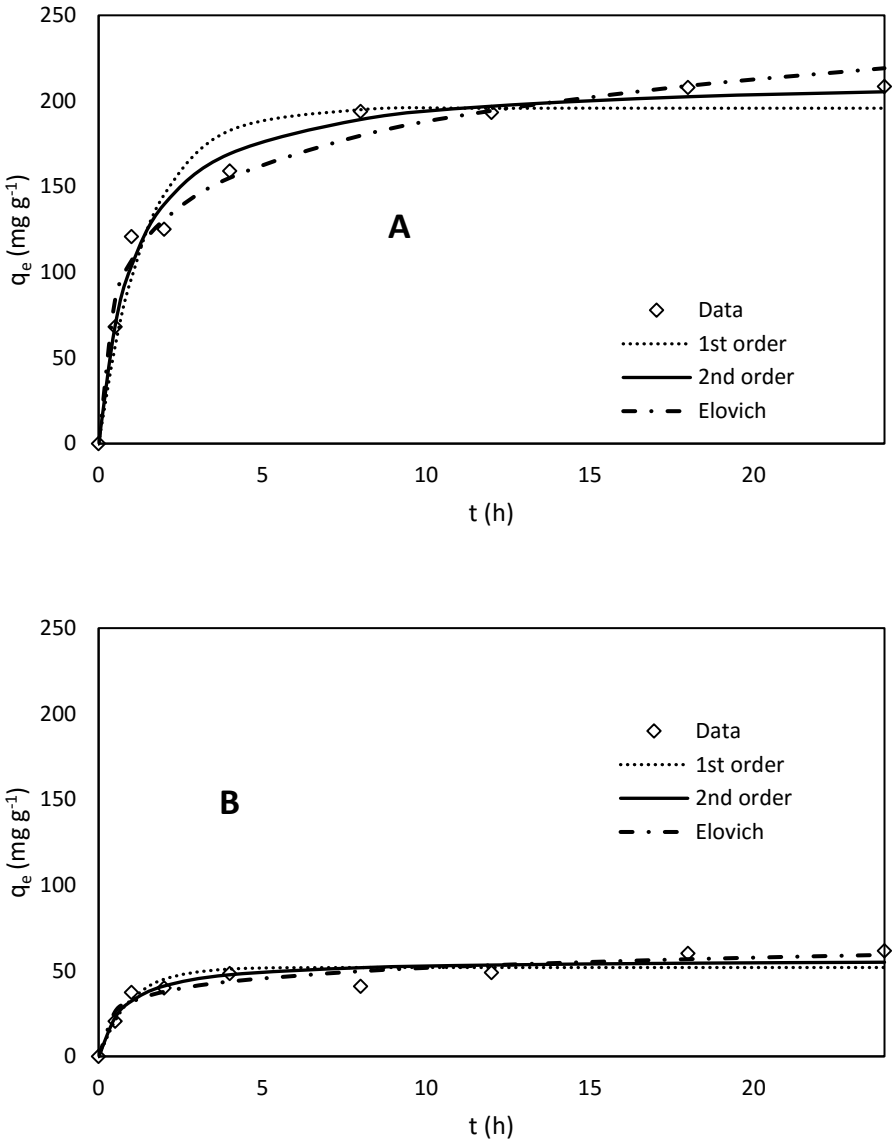

Figure 4-2. Methylene blue adsorption kinetics. A) H_3PO_4 hickory, B) KOH hickory, C) H_3PO_4 peanut, and D) KOH peanut

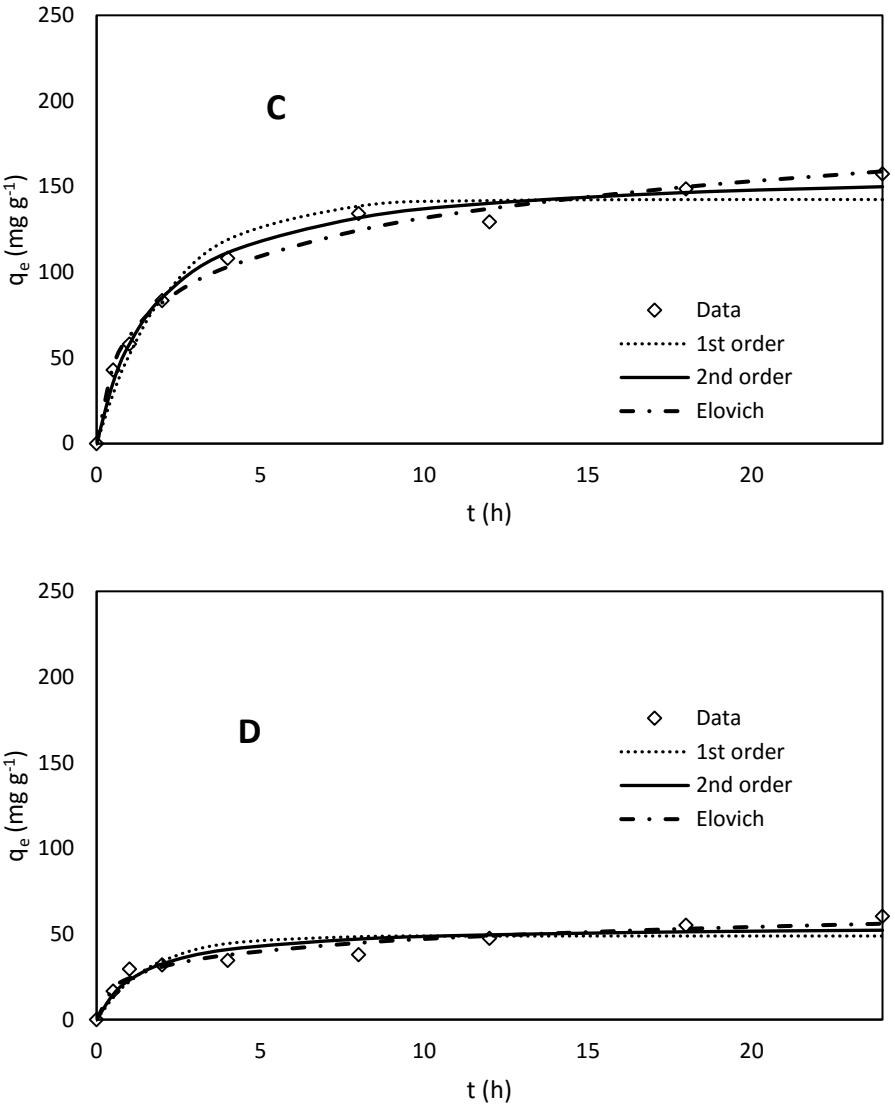

Figure 4-2. Continued

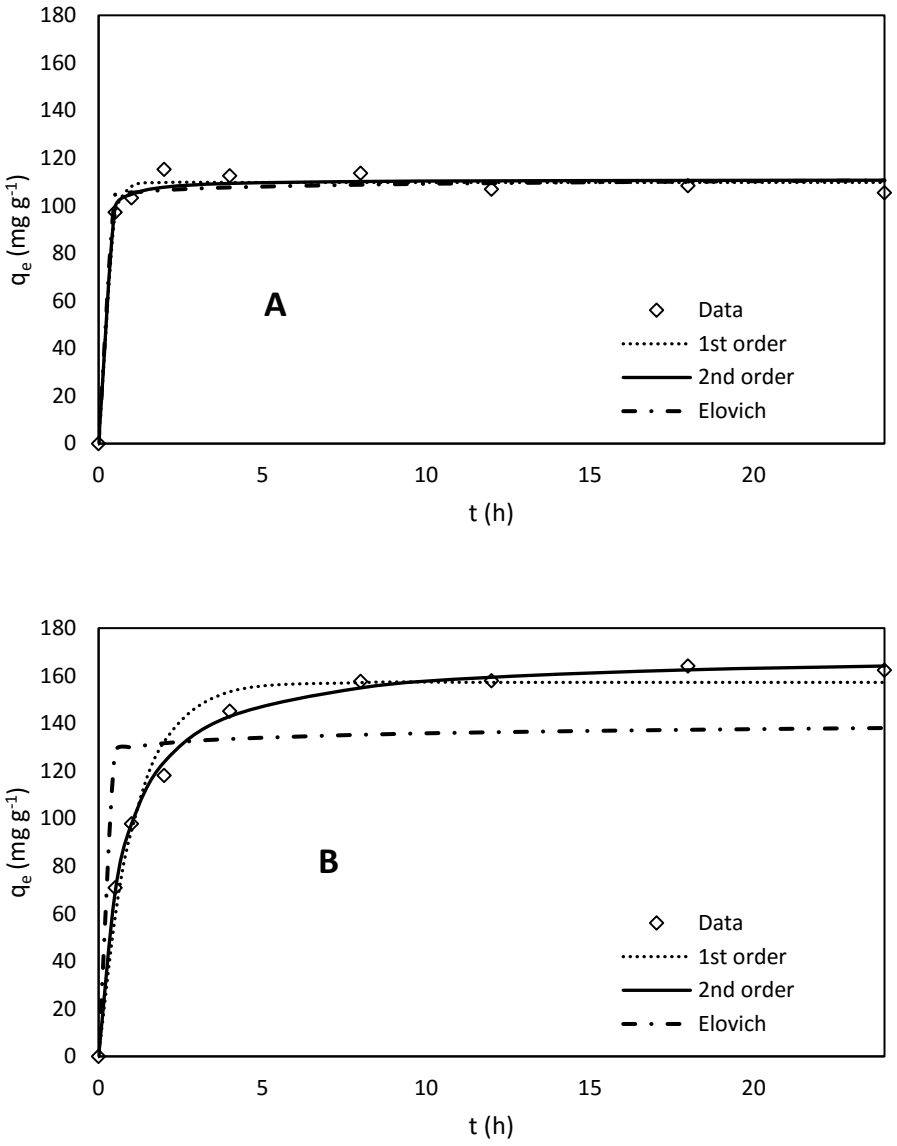

Figure 4-3. Lead adsorption kinetics. A) H_3PO_4 hickory, B) KOH hickory, C) H_3PO_4 peanut, and D) KOH peanut

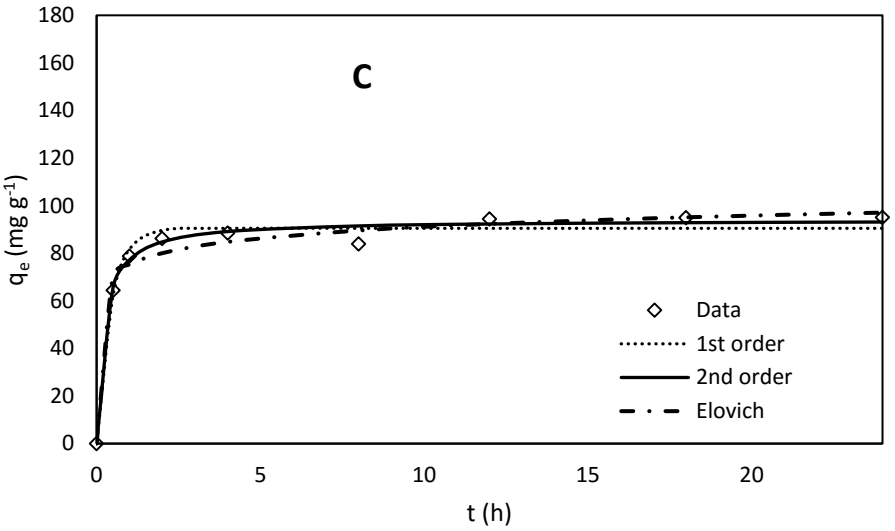

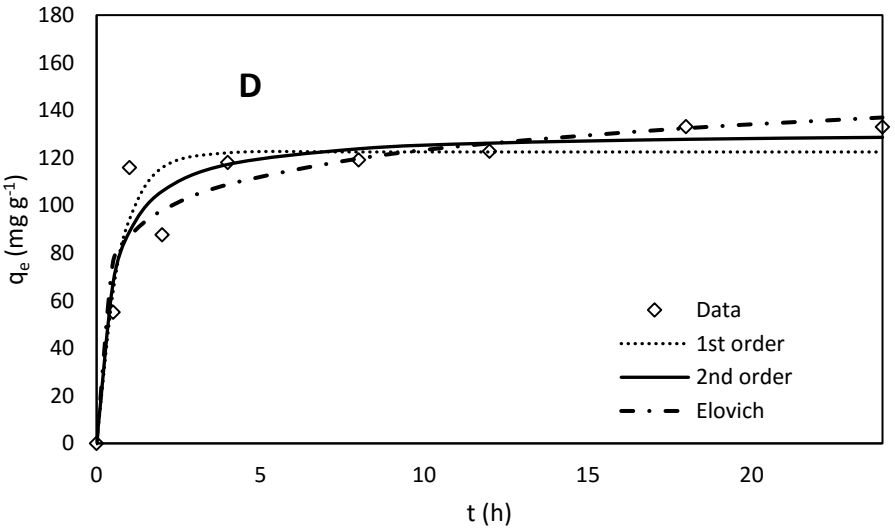

Figure 4-3. Continued

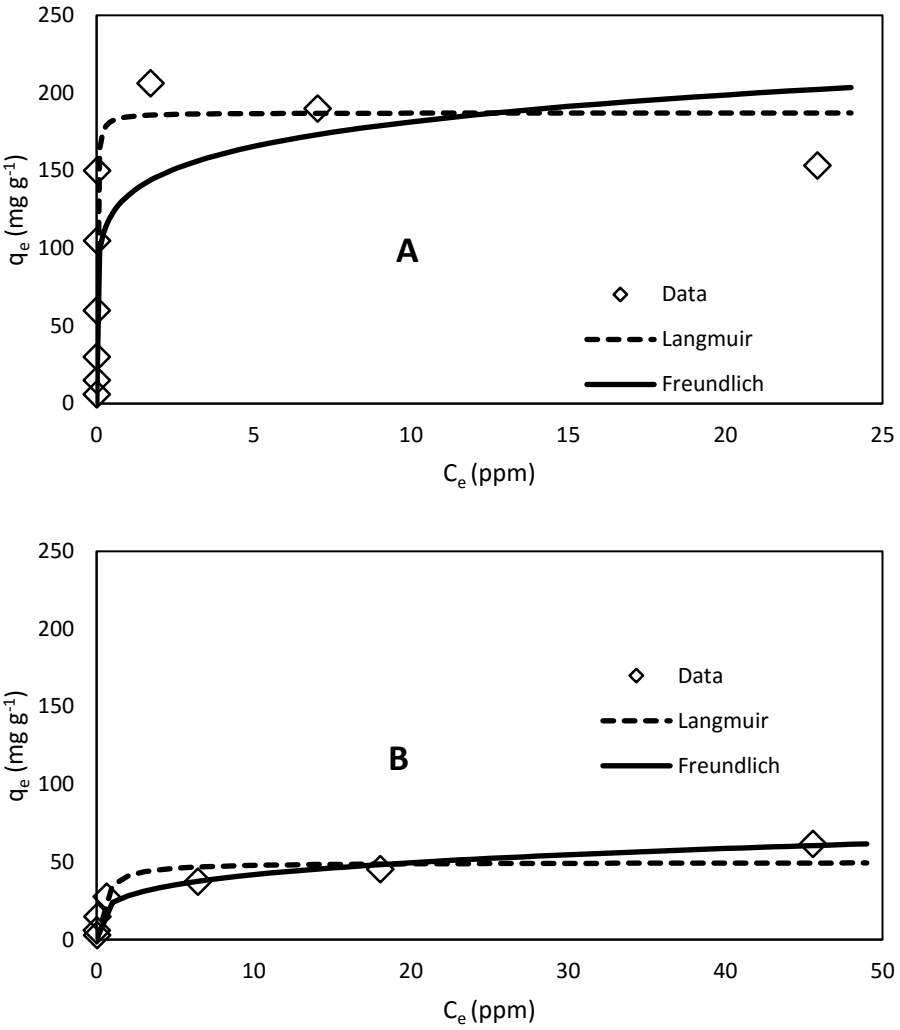

Figure 4-4. Methylene blue adsorption isotherms. A) H_3PO_4 hickory, B) KOH hickory, C) H_3PO_4 peanut, and D) KOH peanut.

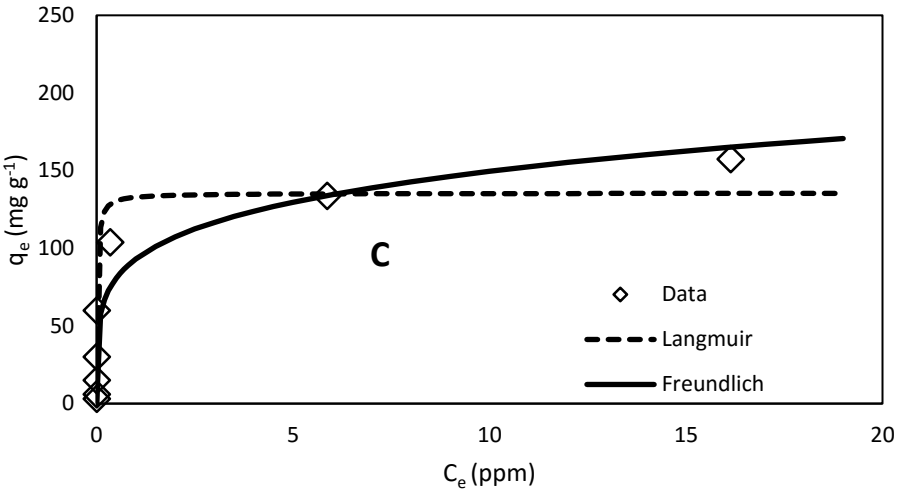

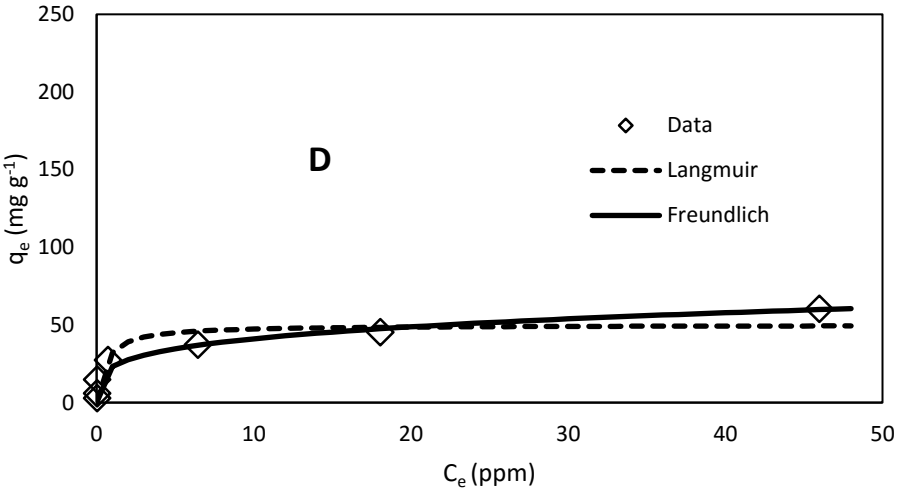

Figure 4-4. Continued

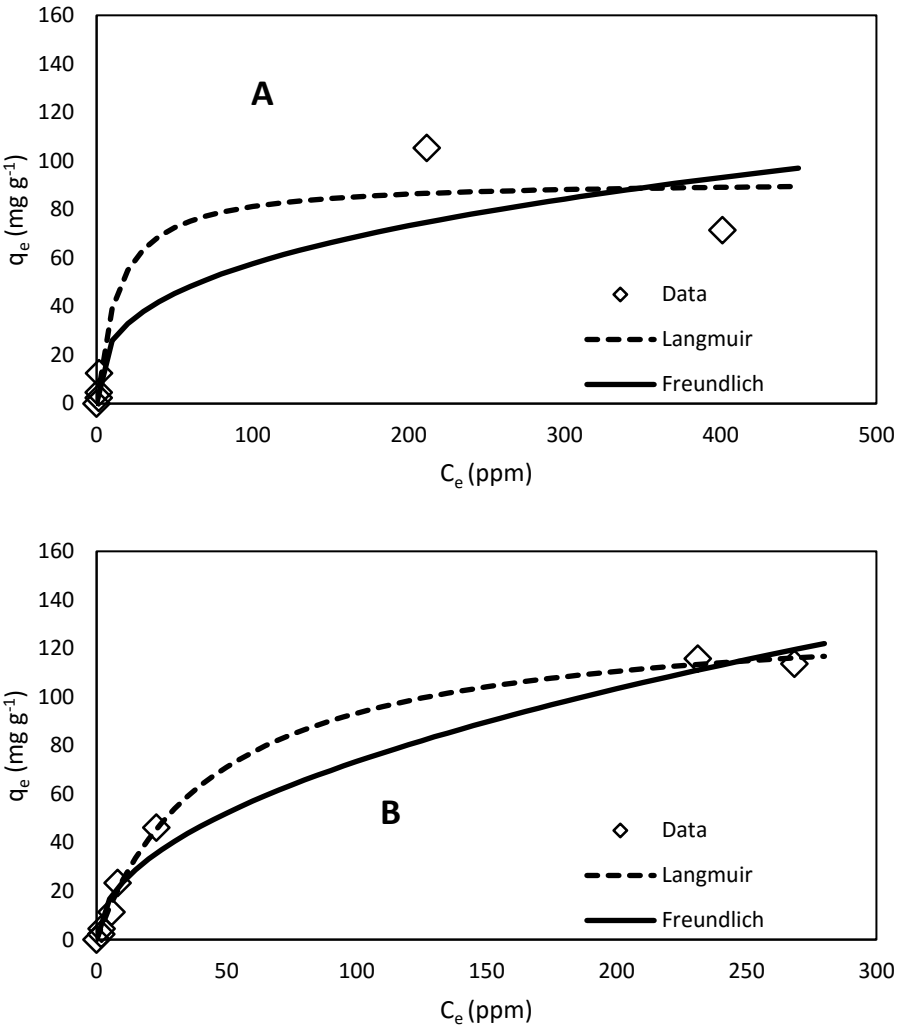

Figure 4-5. Lead adsorption isotherms. A) H_3PO_4 hickory, B) KOH hickory, C) H_3PO_4 peanut, and D) KOH peanut

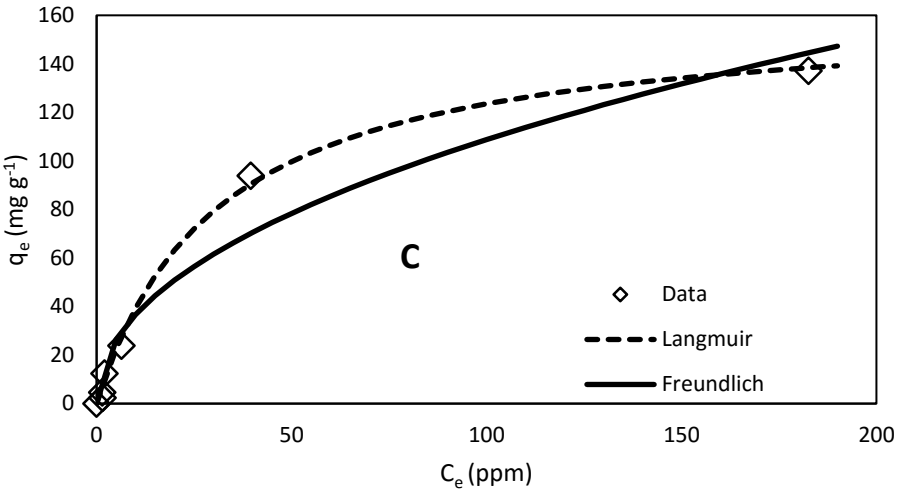

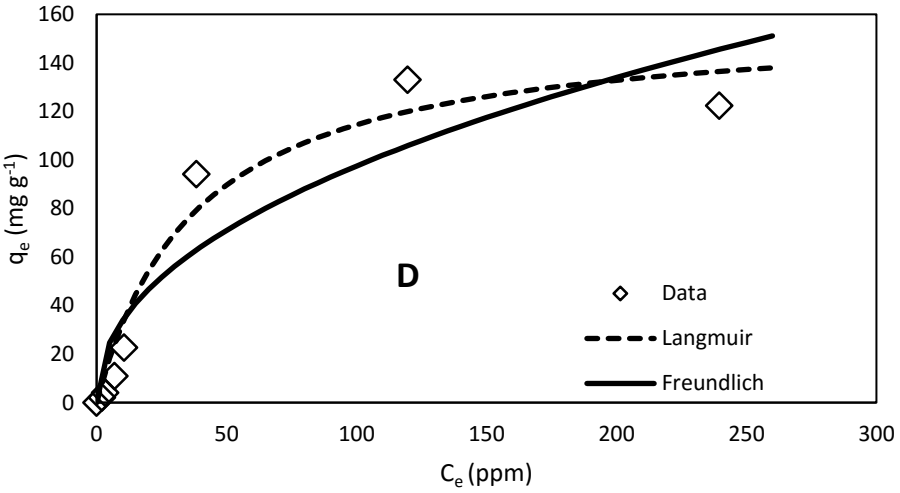

Figure 4-5. Continued

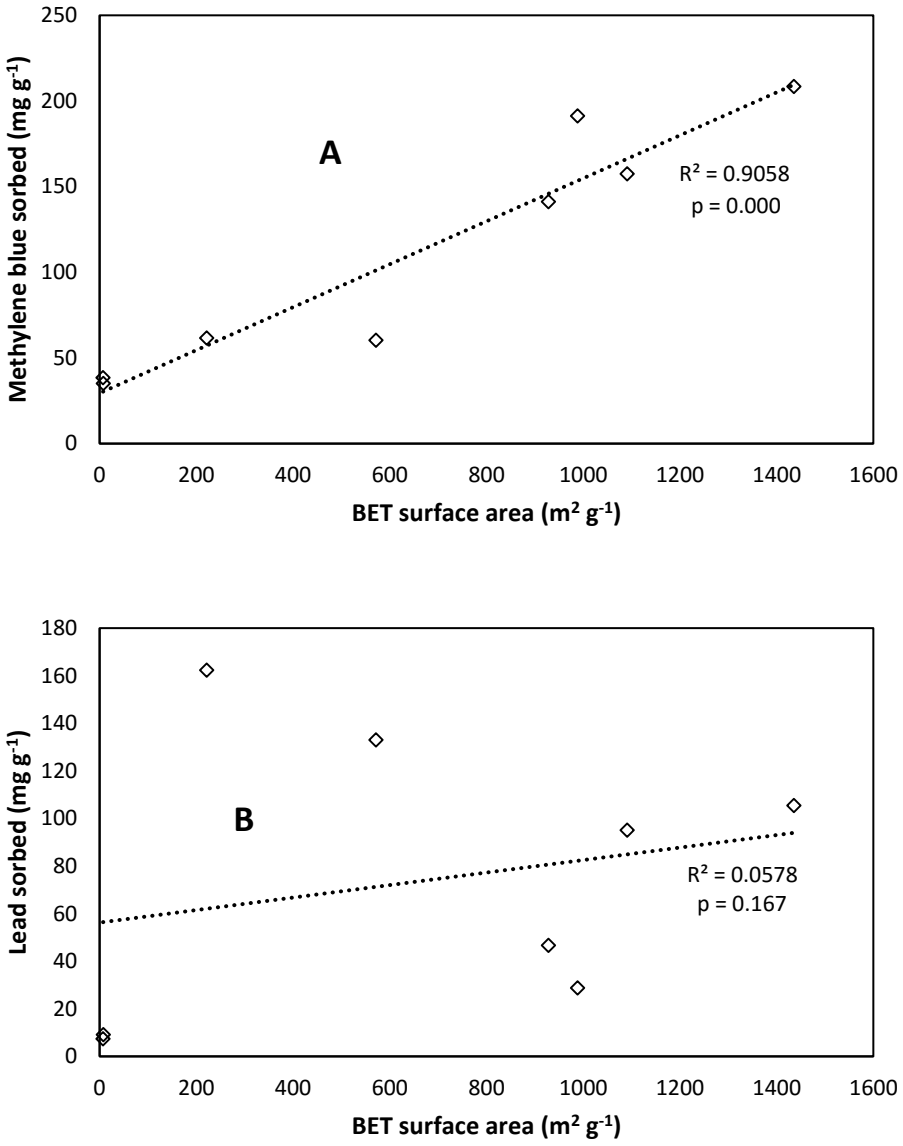

Figure 4-6. Relationship between surface area and amount of contaminant sorbed by raw and AHCs. A) methylene blue and B) Pb

CHAPTER 5
CONCLUDING REMARKS

Summary of Findings

Hydrochars have lower surface area and pore volume as well as higher volatile fractions than biochar, which are characteristics detrimental to environmental applications such as water remediation. However, hydrochar also has desirable properties such as low ash content, since the HTC process releases inorganic elements from the solid into the liquid fraction. This makes it a good feedstock for the production of activated carbon, since the low inorganic elemental content allows for the formation of a highly porous matrix when undergoing activation. Physical and chemical activation were both found to improve the physicochemical properties of hydrochar, especially when it was activated at high temperatures or with H_3PO_4.

Recommendations for Future Studies

Since the physicochemical properties of hydrochar are highly dependent on the feedstock that is used, as well as the processing conditions such as time and temperature and whether or not the hydrochar is later activated. Consequently, different contaminants will have different sorption rates depending on the type of hydrochar used. It is therefore recommended that different combinations of feedstock and processing conditions to be studied in order to find the optimal hydrochar for a certain contaminant.

LIST OF REFERENCES

Abel, S., Peters, A., Trinks, S., Schonsky, H., Facklam, M., Wessolek, G. 2013. Impact of biochar and hydrochar addition on water retention and water repellency of sandy soil. *Geoderma*, **202**, 183-191.

Ahmadpour, A., Do, D.D. 1996. The preparation of active carbons from coal by chemical and physical activation. *Carbon*, **34**(4), 471-479.

Ahmedna, M., Marshall, W.E., Rao, R.M. 2000. Production of granular activated carbons from select agricultural by-products and evaluation of their physical, chemical and adsorption properties. *Bioresource Technology*, **71**(2), 113-123.

Altenor, S., Carene, B., Emmanuel, E., Lambert, J., Ehrhardt, J.J., Gaspard, S. 2009. Adsorption studies of methylene blue and phenol onto vetiver roots activated carbon prepared by chemical activation. *Journal of Hazardous Materials*, **165**(1-3), 1029-1039.

Alvira, P., Tomas-Pejo, E., Ballesteros, M., Negro, M.J. 2010. Pretreatment technologies for an efficient bioethanol production process based on enzymatic hydrolysis: A review. *Bioresource Technology*, **101**(13), 4851-4861.

Angin, D., Altintig, E., Kose, T.E. 2013. Influence of process parameters on the surface and chemical properties of activated carbon obtained from biochar by chemical activation. *Bioresource Technology*, **148**, 542-549.

Aroua, M.K., Leong, S.P.P., Teo, L.Y., Yin, C.Y., Daud, W.M.A.W. 2008. Real-time determination of kinetics of adsorption of lead(II) onto palm shell-based activated carbon using ion selective electrode. *Bioresource Technology*, **99**(13), 5786-5792.

Bacaoui, A., Yaacoubi, A., Dahbi, A., Bennouna, C., Luu, R.P.T., Maldonado-Hodar, F.J., Rivera-Utrilla, J., Moreno-Castilla, C. 2001. Optimization of conditions for the preparation of activated carbons from olive-waste cakes. *Carbon*, **39**(3), 425-432.

Bai, M., Wilske, B., Buegger, F., Bruun, E.W., Bach, M., Frede, H.G., Breuer, L. 2014. Biodegradation measurements confirm the predictive value of the O:C-ratio for biochar recalcitrance. *Journal of Plant Nutrition and Soil Science*, **177**(4), 633-637.

Bargmann, I., Rillig, M.C., Buss, W., Kruse, A., Kuecke, M. 2013. Hydrochar and biochar effects on germination of spring barley. *Journal of Agronomy and Crop Science*, **199**(5), 360-373.

Bargmann, I., Rillig, M.C., Kruse, A., Greef, J.M., Kucke, M. 2014. Effects of hydrochar application on the dynamics of soluble nitrogen in soils and on plant availability. *Journal of Plant Nutrition and Soil Science*, **177**(1), 48-58.

Beck, D.A., Johnson, G.R., Spolek, G.A. 2011. Amending greenroof soil with biochar to affect runoff water quantity and quality. *Environmental Pollution*, **159**(8-9), 2111-2118.

Becker, R., Dorgerloh, U., Helmis, M., Mumme, J., Diakite, M., Nehls, I. 2013. Hydrothermally carbonized plant materials: patterns of volatile organic compounds detected by gas chromatography. *Bioresource Technology*, **130**, 621-628.

Berge, N.D., Ro, K.S., Mao, J.D., Flora, J.R.V., Chappell, M.A., Bae, S.Y. 2011. Hydrothermal carbonization of municipal waste streams. *Environmental Science & Technology*, **45**(13), 5696-5703.

Betancur, M., Martinez, J.D., Murillo, R. 2009. Production of activated carbon by waste tire thermochemical degradation with CO_2. *Journal of Hazardous Materials*, **168**(2-3), 882-887.

Brown, R.A., Kercher, A.K., Nguyen, T.H., Nagle, D.C., Ball, W.P. 2006. Production and characterization of synthetic wood chars for use as surrogates for natural sorbents. *Organic Geochemistry*, **37**(3), 321-333.

Buss, W., Masek, O. 2014. Mobile organic compounds in biochar - A potential source of contamination - Phytotoxic effects on cress seed (*Lepidium sativum*) germination. *Journal of Environmental Management*, **137**, 111-119.

Chang, C.F., Chang, C.Y., Tsai, W.T. 2000. Effects of burn-off and activation temperature on preparation of activated carbon from corn cob agrowaste by CO_2 and steam. *Journal of Colloid and Interface Science*, **232**(1), 45-49.

Chen, S.B., Ma, Y.B., Chen, L., Xian, K. 2010. Adsorption of aqueous Cd^{2+}, Pb^{2+}, Cu^{2+} ions by nano-hydroxyapatite: single- and multi-metal competitive adsorption study. *Geochemical Journal*, **44**(3), 233-239.

Chung, J.W., Foppen, J.W., Gerner, G., Krebs, R., Lens, P.N.L. 2015. Removal of rotavirus and adenovirus from artificial ground water using hydrochar derived from sewage sludge. *Journal of Applied Microbiology*, **119**(3), 876-884.

Chung, J.W., Foppen, J.W., Izquierdo, M., Lens, P.N.L. 2014. Removal of *Escherichia coli* from saturated sand columns supplemented with hydrochar produced from maize. *Journal of Environmental Quality*, **43**(6), 2096-2103.

Dai, L.C., Wu, B., Tan, F.R., He, M.X., Wang, W.G., Qin, H., Tang, X.Y., Zhu, Q.L., Pan, K., Hu, Q.C. 2014. Engineered hydrochar composites for phosphorus removal/recovery: lanthanum doped hydrochar prepared by hydrothermal

carbonization of lanthanum pretreated rice straw. *Bioresource Technology*, **161**, 327-332.

Demirbas, A. 2007. Combustion of biomass. *Energy Sources Part a-Recovery Utilization and Environmental Effects*, **29**(6), 549-561.

Demirbas, A. 2001. Relationships between lignin contents and heating values of biomass. *Energy Conversion and Management*, **42**(2), 183-188.

Ding, L.L., Wang, Z.C., Li, Y.N., Du, Y.L., Liu, H.Q., Guo, Y.P. 2012. A novel hydrochar and nickel composite for the electrochemical supercapacitor electrode material. *Materials Letters*, **74**, 111-114.

Ding, W.C., Dong, X.L., Ime, I.M., Gao, B., Ma, L.Q. 2014a. Pyrolytic temperatures impact lead sorption mechanisms by bagasse biochars. *Chemosphere*, **105**, 68-74.

Ding, Z., Hu, X., Zimmerman, A.R., Gao, B. 2014b. Sorption and cosorption of lead (II) and methylene blue on chemically modified biomass. *Bioresource Technology*, **167**, 569-573.

Dural, M.U., Cavas, L., Papageorgiou, S.K., Katsaros, F.K. 2011. Methylene blue adsorption on activated carbon prepared from *Posidonia oceanica* (L.) dead leaves: Kinetics and equilibrium studies. *Chemical Engineering Journal*, **168**(1), 77-85.

El-Hendawy, A.N.A. 2009. An insight into the KOH activation mechanism through the production of microporous activated carbon for the removal of Pb^{2+} cations. *Applied Surface Science*, **255**(6), 3723-3730.

Fang, J., Gao, B., Chen, J., Zimmerman, A.R. 2015. Hydrochars derived from plant biomass under various conditions: characterization and potential applications and impacts. *Chemical Engineering Journal*, **267**, 253-259.

Fernandez, M.E., Ledesma, B., Roman, S., Bonelli, P.R., Cukierman, A.L. 2015. Development and characterization of activated hydrochars from orange peels as potential adsorbents for emerging organic contaminants. *Bioresource Technology*, **183**, 221-228.

Ferrero, G.A., Fuertes, A.B., Sevilla, M. 2015. From soybean residue to advanced supercapacitors. *Scientific Reports*, **5**.

Fuertes, A.B., Arbestain, M.C., Sevilla, M., Macia-Agullo, J.A., Fiol, S., Lopez, R., Smernik, R.J., Aitkenhead, W.P., Arce, F., Macias, F. 2010. Chemical and structural properties of carbonaceous products obtained by pyrolysis and hydrothermal carbonisation of corn stover. *Australian Journal of Soil Research*, **48**(6-7), 618-626.

Funke, A., Ziegler, F. 2010. Hydrothermal carbonization of biomass: a summary and discussion of chemical mechanisms for process engineering. *Biofuels Bioproducts & Biorefining-Biofpr*, **4**(2), 160-177.

Gajic, A., Koch, H.-J. 2012. Sugar beet (*Beta vulgaris* L.) growth reduction caused by hydrochar is related to nitrogen supply. *Journal of Environmental Quality*, **41**(4), 1067-1075.

Girgis, B.S., Yunis, S.S., Soliman, A.M. 2002. Characteristics of activated carbon from peanut hulls in relation to conditions of preparation. *Materials Letters*, **57**(1), 164-172.

Glaser, B., Lehmann, J., Zech, W. 2002. Ameliorating physical and chemical properties of highly weathered soils in the tropics with charcoal - a review. *Biology and Fertility of Soils*, **35**(4), 219-230.

Guler, C., Copur, Y., Tascioglu, M. 2008. The manufacture of particleboards using mixture of peanut hull (*Arachis hypoqaea* L.) and European black pine (*Pinus nigra* Arnold) wood chips. *Bioresource Technology*, **99**(8), 2893-2897.

Guo, J., Lua, A.C. 1998. Characterization of chars pyrolyzed from oil palm stones for the preparation of activated carbons. *Journal of Analytical and Applied Pyrolysis*, **46**(2), 113-125.

Hammud, H.H., Shmait, A., Hourani, N. 2015. Removal of malachite green from water using hydrothermally carbonized pine needles. *Rsc Advances*, **5**(11), 7909-7920.

Hao, W., Bjorkman, E., Lilliestrale, M., Hedin, N. 2014. Activated carbons for water treatment prepared by phosphoric acid activation of hydrothermally treated beer waste. *Industrial & Engineering Chemistry Research*, **53**(40), 15389-15397.

Harvey, O.R., Kuo, L.J., Zimmerman, A.R., Louchouarn, P., Amonette, J.E., Herbert, B.E. 2012. An index-based approach to assessing recalcitrance and soil carbon sequestration potential of engineered black carbons (biochars). *Environmental Science & Technology*, **46**(3), 1415-1421.

He, C., Giannis, A., Wang, J.-Y. 2013. Conversion of sewage sludge to clean solid fuel using hydrothermal carbonization: hydrochar fuel characteristics and combustion behavior. *Applied Energy*, **111**, 257-266.

Hui, T.S., Zaini, M.A.A. 2015. Potassium hydroxide activation of activated carbon: a commentary. *Carbon Letters*, **16**(4), 275-280.

Inyang, M., Gao, B., Ding, W., Pullammanappallil, P., Zimmerman, A.R., Cao, X. 2011. Enhanced lead sorption by biochar derived from anaerobically digested sugarcane bagasse. *Separation Science and Technology*, **46**(12), 1950-1956.

Inyang, M., Gao, B., Pullammanappallil, P., Ding, W., Zimmerman, A.R. 2010. Biochar from anaerobically digested sugarcane bagasse. *Bioresource Technology*, **101**(22), 8868-8872.

Inyang, M., Gao, B., Yao, Y., Xue, Y.W., Zimmerman, A.R., Pullammanappallil, P., Cao, X.D. 2012. Removal of heavy metals from aqueous solution by biochars derived from anaerobically digested biomass. *Bioresource Technology*, **110**, 50-56.

Inyang, M., Gao, B., Zimmerman, A., Zhang, M., Chen, H. 2014. Synthesis, characterization, and dye sorption ability of carbon nanotube-biochar nanocomposites. *Chemical Engineering Journal*, **236**, 39-46.

Inyang, M., Gao, B., Zimmerman, A., Zhou, Y., Cao, X. 2015. Sorption and cosorption of lead and sulfapyridine on carbon nanotube-modified biochars. *Environmental Science and Pollution Research*, **22**(3), 1868-1876.

Islam, M.A., Kabir, G., Asif, M., Hameed, B.H. 2015. Combustion kinetics of hydrochar produced from hydrothermal carbonisation of Karanj (*Pongamia pinnata*) fruit hulls via thermogravimetric analysis. *Bioresource Technology*, **194**, 14-20.

Jia, X., Wang, Q.H., Cen, K.F., Cheng, L.M. 2016. Sulfur transformation during the pyrolysis of coal mixed with coal ash in a fixed bed reactor. *Fuel*, **177**, 260-267.

Joseph, S., Lehmann, J. 2009. *Biochar for environmental management: science and technology*. London, GB: Earthscan.

Kammann, C., Ratering, S., Eckhard, C., Mueller, C. 2012. Biochar and hydrochar effects on greenhouse gas (carbon dioxide, nitrous oxide, and methane) fluxes from soils. *Journal of Environmental Quality*, **41**(4), 1052-1066.

Kandiyoti, R., Lazaridis, J.I., Dyrvold, B., Weerasinghe, C.R. 1984. Pyrolysis of a $ZnCl_2$-impregnated coal in an inert atmosphere. *Fuel*, **63**(11), 1583-1587.

Kang, S.M., Li, X.H., Fan, J., Chang, J. 2012. Characterization of hydrochars produced by hydrothermal carbonization of lignin, cellulose, d-xylose, and wood meal. *Industrial & Engineering Chemistry Research*, **51**(26), 9023-9031.

Kannan, N., Sundaram, M.M. 2001. Kinetics and mechanism of removal of methylene blue by adsorption on various carbons - a comparative study. *Dyes and Pigments*, **51**(1), 25-40.

Kim, D., Lee, K., Park, K.Y. 2014. Hydrothermal carbonization of anaerobically digested sludge for solid fuel production and energy recovery. *Fuel*, **130**, 120-125.

Kloss, S., Zehetner, F., Dellantonio, A., Hamid, R., Ottner, F., Liedtke, V., Schwanninger, M., Gerzabek, M.H., Soja, G. 2012. Characterization of slow pyrolysis biochars: effects of feedstocks and pyrolysis temperature on biochar properties. *Journal of Environmental Quality*, **41**(4), 990-1000.

Kobya, M., Demirbas, E., Senturk, E., Ince, M. 2005. Adsorption of heavy metal ions from aqueous solutions by activated carbon prepared from apricot stone. *Bioresource Technology*, **96**(13), 1518-1521.

Kumar, B.G.P., Shivakamy, K., Miranda, L.R., Velan, M. 2006. Preparation of steam activated carbon from rubberwood sawdust (*Hevea brasiliensis*) and its adsorption kinetics. *Journal of Hazardous Materials*, **136**(3), 922-929.

Largitte, L., Gervelas, S., Tant, T., Dumesnil, P.C., Hightower, A., Yasami, R., Bercion, Y., Lodewyckx, P. 2014. Removal of lead from aqueous solutions by adsorption with surface precipitation. *Adsorption-Journal of the International Adsorption Society*, **20**(5-6), 689-700.

Lehtikangas, P. 2000. Storage effects on pelletised sawdust, logging residues and bark. *Biomass & Bioenergy*, **19**(5), 287-293.

Liao, R., Gao, B., Fang, J. 2013. Invasive plants as feedstock for biochar and bioenergy production. *Bioresource Technology*, **140**, 439-442.

Libra, J.A., Ro, K.S., Kammann, C., Funke, A., Berge, N.D., Neubauer, Y., Titirici, M.M., Fuhner, C., Bens, O., Kern, J., Emmerich, K.H. 2011. Hydrothermal carbonization of biomass residuals: a comparative review of the chemistry, processes and applications of wet and dry pyrolysis. *Biofuels*, **2**(1), 71-106.

Lillo-Rodenas, M.A., Juan-Juan, J., Cazorla-Amoros, D., Linares-Solano, A. 2004. About reactions occurring during chemical activation with hydroxides. *Carbon*, **42**(7), 1371-1375.

Liu, Z., Quek, A., Balasubramanian, R. 2014. Preparation and characterization of fuel pellets from woody biomass, agro-residues and their corresponding hydrochars. *Applied Energy*, **113**, 1315-1322.

Liu, Z.G., Zhang, F.S. 2009. Removal of lead from water using biochars prepared from hydrothermal liquefaction of biomass. *Journal of Hazardous Materials*, **167**(1-3), 933-939.

Lu, X., Jordan, B., Berge, N.D. 2012. Thermal conversion of municipal solid waste via hydrothermal carbonization: comparison of carbonization products to products from current waste management techniques. *Waste Management*, **32**(7), 1353-1365.

Lua, A.C., Yang, T., Guo, J. 2004. Effects of pyrolysis conditions on the properties of activated carbons prepared from pistachio-nut shells. *Journal of Analytical and Applied Pyrolysis*, **72**(2), 279-287.

Maga, J.A. 1986. Polycyclic aromatic hydrocarbon (PAH) composition of mesquite (*Prosopis fuliflora*) smoke and grilled beef. *Journal of Agricultural and Food Chemistry*, **34**(2), 249-251.

Malghani, S., Gleixner, G., Trumbore, S.E. 2013. Chars produced by slow pyrolysis and hydrothermal carbonization vary in carbon sequestration potential and greenhouse gases emissions. *Soil Biology and Biochemistry*, **62**, 137-146.

Mestre, A.S., Tyszko, E., Andrade, M.A., Galhetas, M., Freire, C., Carvalho, A.P. 2015. Sustainable activated carbons prepared from a sucrose-derived hydrochar: remarkable adsorbents for pharmaceutical compounds. *Rsc Advances*, **5**(25), 19696-19707.

Mohan, D., Sarswat, A., Ok, Y.S., Pittman, C.U. 2014. Organic and inorganic contaminants removal from water with biochar, a renewable, low cost and sustainable adsorbent - a critical review. *Bioresource Technology*, **160**, 191-202.

Mukherjee, A., Zimmerman, A.R., Harris, W. 2011. Surface chemistry variations among a series of laboratory-produced biochars. *Geoderma*, **163**(3-4), 247-255.

Mumme, J., Eckervogt, L., Pielert, J., Diakite, M., Rupp, F., Kern, J. 2011. Hydrothermal carbonization of anaerobically digested maize silage. *Bioresource Technology*, **102**(19), 9255-9260.

Namasivayam, C., Kavitha, D. 2002. Removal of Congo Red from water by adsorption onto activated carbon prepared from coir pith, an agricultural solid waste. *Dyes and Pigments*, **54**(1), 47-58.

Ngernyen, Y., Tangsathitkulchai, C., Tangsathitkulchai, M. 2006. Porous properties of activated carbon produced from eucalyptus and wattle wood by carbon dioxide activation. *Korean Journal of Chemical Engineering*, **23**(6), 1046-1054.

Oliveira, I., Blohse, D., Ramke, H.G. 2013. Hydrothermal carbonization of agricultural residues. *Bioresource Technology*, **142**, 138-146.

Parshetti, G.K., Chowdhury, S., Balasubramanian, R. 2014. Hydrothermal conversion of urban food waste to chars for removal of textile dyes from contaminated waters. *Bioresource Technology*, **161**, 310-319.

Qian, K.Z., Kumar, A., Patil, K., Bellmer, D., Wang, D.H., Yuan, W.Q., Huhnke, R.L. 2013. Effects of biomass feedstocks and gasification conditions on the physiochemical properties of char. *Energies*, **6**(8), 3972-3986.

Reza, M.T., Lynam, J.G., Vasquez, V.R., Coronella, C.J. 2012. Pelletization of biochar from hydrothermally carbonized wood. *Environmental Progress & Sustainable Energy*, **31**(2), 225-234.

Reza, M.T., Wirth, B., Lueder, U., Werner, M. 2014. Behavior of selected hydrolyzed and dehydrated products during hydrothermal carbonization of biomass. *Bioresource Technology*, **169**, 352-361.

Ro, K.S., Novak, J.M., Johnson, M.G., Szogi, A.A., Libra, J.A., Spokas, K.A., Bae, S. 2016. Leachate water quality of soils amended with different swine manure-based amendments. *Chemosphere*, **142**, 92-99.

Rondon, M.A., Lehmann, J., Ramirez, J., Hurtado, M. 2007. Biological nitrogen fixation by common beans (*Phaseolus vulgaris* L.) increases with bio-char additions. *Biology and Fertility of Soils*, **43**(6), 699-708.

Ruan, S.B., Wan, J.Y., Fu, Y., Han, K., Li, X., Chen, J.T., Zhang, Q.Y., Shen, S., He, Q., Gao, H.L. 2014. PEGylated fluorescent carbon nanoparticles for noninvasive heart imaging. *Bioconjugate Chemistry*, **25**(6), 1061-1068.

Salas-Enriquez, B.G., Torres-Huerta, A.M., Conde-Barajas, E., Dominguez-Crespo, M.A., Diaz-Garcia, L., Negrete-Rodriguez, M.D.X. 2016. Activated carbon production from the *Guadua amplexifolia* using a combination of physical and chemical activation. *Journal of Thermal Analysis and Calorimetry*, **124**(3), 1383-1398.

Schimmelpfennig, S., Muller, C., Grunhage, L., Koch, C., Kammann, C. 2014. Biochar, hydrochar and uncarbonized feedstock application to permanent grassland-effects on greenhouse gas emissions and plant growth. *Agriculture Ecosystems & Environment*, **191**, 39-52.

Sevilla, M., Fuertes, A.B. 2009. The production of carbon materials by hydrothermal carbonization of cellulose. *Carbon*, **47**(9), 2281-2289.

Spokas, K.A. 2010. Review of the stability of biochar in soils: predictability of O:C molar ratios. *Carbon Management*, **1**(2), 289-303.

Stemann, J., Putschew, A., Ziegler, F. 2013. Hydrothermal carbonization: process water characterization and effects of water recirculation. *Bioresource Technology*, **143**, 139-146.

Suhas, Carrott, P.J.M., Carrott, M.M.L.R. 2007. Lignin - from natural adsorbent to activated carbon: a review. *Bioresource Technology*, **98**(12), 2301-2312.

Sun, K., Ro, K., Guo, M., Novak, J., Mashayekhi, H., Xing, B. 2011. Sorption of bisphenol A, 17 alpha-ethinyl estradiol and phenanthrene on thermally and hydrothermally produced biochars. *Bioresource Technology*, **102**(10), 5757-5763.

Sun, K., Tang, J., Gong, Y., Zhang, H. 2015. Characterization of potassium hydroxide (KOH) modified hydrochars from different feedstocks for enhanced removal of heavy metals from water. *Environmental Science and Pollution Research*, **22**(21), 16640-16651.

Sun, Y.N., Gao, B., Yao, Y., Fang, J.N., Zhang, M., Zhou, Y.M., Chen, H., Yang, L.Y. 2014. Effects of feedstock type, production method, and pyrolysis temperature on biochar and hydrochar properties. *Chemical Engineering Journal*, **240**, 574-578.

Takaya, C.A., Fletcher, L.A., Singh, S., Anyikude, K.U., Ross, A.B. 2016. Phosphate and ammonium sorption capacity of biochar and hydrochar from different wastes. *Chemosphere*, **145**, 518-527.

Uchimiya, M., Chang, S., Klasson, K.T. 2011. Screening biochars for heavy metal retention in soil: role of oxygen functional groups. *Journal of Hazardous Materials*, **190**(1-3), 432-441.

Valix, M., Cheung, W.H., McKay, G. 2004. Preparation of activated carbon using low temperature carbonisation and physical activation of high ash raw bagasse for acid dye adsorption. *Chemosphere*, **56**(5), 493-501.

Van Zwieten, L., Kimber, S., Morris, S., Chan, K.Y., Downie, A., Rust, J., Joseph, S., Cowie, A. 2010. Effects of biochar from slow pyrolysis of papermill waste on agronomic performance and soil fertility. *Plant and Soil*, **327**(1-2), 235-246.

Verheijen, F., Jeffery, S., Bastos, A.C., Velde, M.v.d., Diafas, I. 2009. *Biochar application to soils - a critical scientific review of effects on soil properties, processes and functions*. EUR 24099 EN, Office for the Official Publications of the European Communities, Luxemburg, 149pp.

Wagner, W. 1973. New vapor-pressure measurements for argon and nitrogen and a new method for establishing rational vapor-pressure equations. *Cryogenics*, **13**(8), 470-482.

Wang, S.B., Zhu, Z.H., Coomes, A., Haghseresht, F., Lu, G.Q. 2005. The physical and surface chemical characteristics of activated carbons and the adsorption of methylene blue from wastewater. *Journal of Colloid and Interface Science*, **284**(2), 440-446.

Xue, Y., Gao, B., Yao, Y., Inyang, M., Zhang, M., Zimmerman, A.R., Ro, K.S. 2012. Hydrogen peroxide modification enhances the ability of biochar (hydrochar) produced from hydrothermal carbonization of peanut hull to remove aqueous heavy metals: Batch and column tests. *Chemical Engineering Journal*, **200**, 673-680.

Yao, Y., Gao, B., Chen, J., Yang, L. 2013a. Engineered biochar reclaiming phosphate from aqueous solutions: mechanisms and potential application as a slow-release fertilizer. *Environmental Science & Technology*, **47**(15), 8700-8708.

Yao, Y., Gao, B., Chen, J., Zhang, M., Inyang, M., Li, Y., Alva, A., Yang, L. 2013b. Engineered carbon (biochar) prepared by direct pyrolysis of Mg-accumulated tomato tissues: characterization and phosphate removal potential. *Bioresource Technology*, **138**, 8-13.

Yao, Y., Gao, B., Fang, J., Zhang, M., Chen, H., Zhou, Y., Creamer, A.E., Sun, Y., Yang, L. 2014. Characterization and environmental applications of clay-biochar composites. *Chemical Engineering Journal*, **242**, 136-143.

Yao, Y., Gao, B., Inyang, M., Zimmerman, A.R., Cao, X.D., Pullammanappallil, P., Yang, L.Y. 2011. Removal of phosphate from aqueous solution by biochar derived from anaerobically digested sugar beet tailings. *Journal of Hazardous Materials*, **190**(1-3), 501-507.

Yuan, J.H., Xu, R.K., Zhang, H. 2011. The forms of alkalis in the biochar produced from crop residues at different temperatures. *Bioresource Technology*, **102**(3), 3488-3497.

Zhang, M., Gao, B. 2013. Removal of arsenic, methylene blue, and phosphate by biochar/AlOOH nanocomposite. *Chemical Engineering Journal*, **226**, 286-292.

Zhang, M., Gao, B., Yao, Y., Inyang, M. 2013. Phosphate removal ability of biochar/MgAl-LDH ultra-fine composites prepared by liquid-phase deposition. *Chemosphere*, **92**(8), 1042-1047.

Zhang, M., Gao, B., Yao, Y., Xue, Y., Inyang, M. 2012a. Synthesis of porous MgO-biochar nanocomposites for removal of phosphate and nitrate from aqueous solutions. *Chemical Engineering Journal*, **210**, 26-32.

Zhang, M., Gao, B., Yao, Y., Xue, Y., Inyang, M. 2012b. Synthesis, characterization, and environmental implications of graphene-coated biochar. *Science of the Total Environment*, **435**, 567-572.

Zhang, T.Y., Walawender, W.P., Fan, L.T., Fan, M., Daugaard, D., Brown, R.C. 2004. Preparation of activated carbon from forest and agricultural residues through CO2 activation. *Chemical Engineering Journal*, **105**(1-2), 53-59.

Zhou, Y., Gao, B., Zimmerman, A.R., Fang, J., Sun, Y., Cao, X. 2013. Sorption of heavy metals on chitosan-modified biochars and its biological effects. *Chemical Engineering Journal*, **231**, 512-518.

Zimmerman, A.R. 2010. Abiotic and microbial oxidation of laboratory-produced black carbon (biochar). *Environmental Science & Technology*, **44**(4), 1295-1301.

Zimmerman, A.R., Gao, B., Ahn, M.Y. 2011. Positive and negative carbon mineralization priming effects among a variety of biochar-amended soils. *Soil Biology & Biochemistry*, **43**(6), 1169-1179.

BIOGRAPHICAL SKETCH

June Fang received her Bachelor of Science degree in environmental earth science with a minor in energy and water sustainability at Rice University in 2011. In 2012, she came to the University of Florida to pursue a doctorate degree in agricultural and biological engineering, where she had also participated in an NSF REU program during the summer of 2010.